

TABLE I. DXCPN Card Entries

Cell	Probability
2	0.001
3	0.001
4	0.001
5	0.001
6	0.01
7	0.01
8	0.01
9	0.01
10	0.01
11	0.01
12	0.015
13	0.02
14	0.04
15	0.08
16	0.2
17	0.4
18	1
19	1
20	VOID, no collisions
21	INSIDE SPHERE, no DXTRAN game played
22	VOID, no collisions

detector can be used instead of a point detector. The ring detector estimates the average flux on a ring rather than the flux at a point, but because the sample problem is symmetric, these tallies (on average) will be the same. The ring detector gives lower variance estimates than the point detector, especially if, unlike the sample problem, the detectors are embedded in a scattering medium. On average, collisions are closer to a ring detector than to a point detector, so the ring detector better samples the close collisions that tend to trounce the point detector statistics. Particularly important in some problems, but not this sample problem, is that the ring detector has finite variance even in a scattering medium. The point detector does not.

For the sample problem, I chose a ring of radius 200 cm about the y-axis such that the ring detector went through the point where the point detector had been. The results are shown in Fig. 19. Note that everything is about the same as with the point detector, except that the ring detector's FOM has increased from 34 (Fig. 18) to 41. More difference would be seen if the detector were in, or close to, cell 21.

XII. BIASING THE SOURCE

- No attempt has been made to bias the source although
1. source particles moving downward ($-\hat{y}$) are unimportant because they immediately escape, and

2. high-energy source particles (14 MeV) penetrate better than low-energy source particles (2 MeV) so are more important.

MCNP has two types of source direction bias that will be employed, followed by source energy bias.

A. Cone Bias

Cone biasing, a type of angular biasing, is illustrated in Fig. 20. A cone is specified that divides the angular domain into two pieces, one inside and one outside the cone. The user then specifies the fraction of particles to be started inside the cone and outside the cone. All particles started inside are of one weight; all particles started outside are of another (in the absence of other source biasing, for example, source energy biasing). One consequence of all particles inside the cone having one weight and all particles outside the cone having a different one is that there is weight discontinuity at the cone surface. This weight discontinuity should be considered before using heavy cone biasing. Exponential source biasing, discussed in Sec. XII-B, should be considered if the cone bias weight discontinuity is too large.

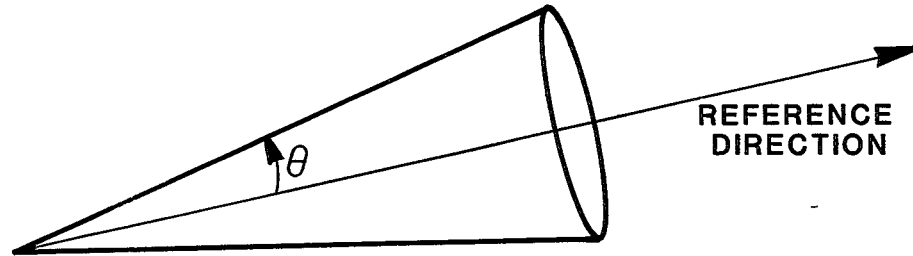
Figure 21 shows the effects of using cone biasing to send 99% of the particles in the $+\hat{y}$ half-space. Note that the FOMs are roughly the same as before cone biasing. Indeed, the only major difference is that the number of particles started has dropped by a factor of 2, as might be expected because almost all of the time is spent following particles moving in the $+\hat{y}$ direction. No improvement occurred because the source sampling is very fast and it does not take long for source particles going in $-\hat{y}$ direction to die. Stated another way, both runs had about 6000 particles sampled in the $+\hat{y}$ direction, so both runs gave roughly the same results. The cone bias saved only a small amount of time *not* sampling the 6000 particles that would have gone in the $-\hat{y}$ direction.

B. Exponential Source Biasing

In addition to the cone bias just discussed, MCNP has a continuous angle bias called exponential source biasing because the sampled density is an exponential in the cosine of the angle with respect to a specified reference direction. That is, the probability density function for exponential source biasing is

$$p(\mu) = Ce^{k\mu} \quad (\mu = \cos \theta),$$

where k = user-selected biasing parameter $0.01 \leq k \leq 3.5$ and C = normalization constant $C = k/(e^k - e^{-k})$. Table II shows how the particle weight at some angles varies with k . Note that although the exponential angle biasing has no weight discontinuities, large weight fluctuations can be introduced by setting k too large. For



SPECIFY:

1. $\nu = \cos(\theta)$ FOR FAVORED CONE
2. FRACTION OF PARTICLES STARTED INSIDE CONE

COMMENTS:

1. ALL PARTICLES INSIDE CONE HAVE IDENTICAL WEIGHTS
2. ALL PARTICLES OUTSIDE CONE HAVE IDENTICAL WEIGHTS

Fig. 20. Cone Bias.

example, with $k = 3.5$, the weight ratio between $\theta = 0^\circ$ and $\theta = 180^\circ$ is 1094.

I chose the exponential biasing parameter $k = 2$ on the basis of Table II. Recall that any particle departing the source in the $-\hat{y}$ direction ($\theta > 90^\circ$) will be killed immediately. Thus I confined my attention to the weight variation between $\theta = 0^\circ$ and $\theta = 90^\circ$. For $k = 2$, there is a factor of about 8 fluctuation in weight between $\theta = 0^\circ$ and 90° . Experience indicated that a source particle at $\theta = 0^\circ$ might be eight times as important as a source particle at 90° . Maybe 8 was not a particularly good guess, but I would be highly surprised if the "right" ratio were not within a factor of 3.

Figure 22 shows the effects of exponential source biasing. The FOM columns indicate no drastic change and probably a small degradation in calculational efficiency. Thus source angle biasing did not appear effective for the sample problem. However, a conference participant (John Hendricks) suggested that source angle biasing might have worked better with the weight window technique (Sec. XIII) than with the geometry splitting/Russian roulette technique used here. I shall have more to say about Hendricks' suggestion in Sec. XIV.

C. Source Alteration in the Sample Problem

The runs so far have been with an isotropic source with the following energy distribution:

1. 25% of the particles started at 2 MeV.
2. 25% of the particles uniformly distributed between 2 MeV and 14 MeV.
3. 50% of the particles at 14 MeV.

In preparing this report I had intended to use 50% at 2 MeV and 50% at 14 MeV, so source energy biasing could be tried on a simple case. After discovering the input error that arose from using the first energy distribution above rather than the second, I decided that if the source was going to change anyway, a more interesting source could be used instead of the second distribution. All subsequent runs have 95% at 2 MeV and 5% at 14 MeV, making it easy to demonstrate biasing in energy. Note that this spectrum is much softer than the one used before, so tallies will drop and the calculation will therefore be more difficult than before.

The first run with the new source uses all the successful variance reduction techniques (with identical parameters) used for the sample problem with the old source except energy roulette. Specifically, the first run with the new source uses

CELL PROGR PROBL	TRACKS ENTERING	POPULATION	COLLISIONS	COLLISIONS * WEIGHT (PER HISTORY)	NUMBER WEIGHTED ENERGY	FLUX WEIGHTED ENERGY	AVERAGE TRACK WEIGHT (RELATIVE)	AVERAGE TRACK MFP (CM)
2 2	6605	6406	14695	1.9658E+00	2.0739E+00	6.0195E+00	6.6003E-01	6.8857E+00
3 3	5640	5220	12812	1.1148E+00	1.1286E+00	3.9936E+00	8.5805E-01	5.9323E+00
4 4	5330	4934	12290	6.0646E-01	8.2161E-01	3.2831E+00	1.0041E+00	5.5831E+00
5 5	5074	4718	11282	2.6844E-01	7.9748E-01	3.1278E+00	1.0501E+00	5.6114E+00
6 6	4681	4306	10143	1.2446E-01	8.0250E-01	2.9926E+00	1.0843E+00	5.6203E+00
7 7	4464	4090	10110	6.6575E-02	7.3839E-01	2.7183E+00	1.1594E+00	5.4194E+00
8 8	4115	3799	9267	3.0420E-02	7.6131E-01	2.6942E+00	1.1432E+00	5.5398E+00
9 9	4161	3858	9322	1.4746E-02	7.1952E-01	2.5393E+00	1.1895E+00	5.4467E+00
10 10	4302	3985	9585	7.4080E-03	7.0524E-01	2.4389E+00	1.2186E+00	5.4138E+00
11 11	4424	4105	10231	3.5739E-03	6.7007E-01	2.3164E+00	1.2352E+00	5.3339E+00
12 12	4498	4157	10257	1.7292E-03	6.8539E-01	2.2800E+00	1.2411E+00	5.3575E+00
13 13	4683	4329	10229	8.0300E-04	6.7528E-01	2.2984E+00	1.2314E+00	5.4287E+00
14 14	4671	4340	10751	3.8336E-04	6.9439E-01	2.2499E+00	1.2361E+00	5.4183E+00
15 15	4614	4271	10494	1.7918E-04	6.6366E-01	2.1724E+00	1.2611E+00	5.3735E+00
16 16	4721	4384	10802	8.6520E-05	6.0949E-01	2.0604E+00	1.3078E+00	5.2351E+00
17 17	4653	4309	11002	3.9905E-05	6.1264E-01	1.9942E+00	1.3234E+00	5.2048E+00
18 18	4359	4060	9952	1.6436E-05	6.4482E-01	2.0619E+00	1.2907E+00	5.3094E+00
19 19	3916	3823	8868	6.4892E-06	6.8815E-01	2.1795E+00	1.2469E+00	5.4875E+00
20 20	4486	16134	0	0.	1.4905E+00	3.5288E+00	3.9695E-01	1.0000+123
21 21	13367	26736	13672	6.7894E-11	1.5740E+00	3.9432E+00	5.5103E-04	7.2941E+02
22 22	1063	1063	0	0.	7.2051E-01	1.9923E+00	1.8421E-05	1.0000+123
TOTAL	103827	123027	205764	4.2059E+00				

ROUGHLY
THE SAME

NPS	TALLY 1			TALLY 4			TALLY 5		
	MEAN	ERROR	FOM	MEAN	ERROR	FOM	MEAN	ERROR	FOM
1000	9.62664E-07	.2587	28	1.52991E-13	.2256	37	8.70445E-17	.2290	36
2000	8.86500E-07	.1777	33	1.39145E-13	.1591	41	8.47413E-17	.1652	38
3000	7.21686E-07	.1543	32	1.18189E-13	.1358	41	7.33522E-17	.1420	38
4000	6.89222E-07	.1295	34	1.19786E-13	.1124	45	7.30212E-17	.1185	41
5000	6.49018E-07	.1225	31	1.15679E-13	.1031	44	7.00919E-17	.1077	40
6000	6.87974E-07	.1084	32	1.23255E-13	.0924	45	7.42021E-17	.0972	40
6049	6.82401E-07	.1084	32	1.22481E-13	.0922	45	7.37452E-17	.0970	40

DUMP NO. 2 ON FILE RUNTPF NPS = 6049 CTM = 2.60

AS EXPECTED, ABOUT HALF

CONCLUSION: NO IMPROVEMENT BECAUSE DID NOT TAKE LONG FOR SOURCE
PARTICLES GOING IN -y DIRECTION TO DIE.

Fig. 21. Cone biasing—99% in +y half-space.

1. energy cutoff,
2. geometry splitting/Russian roulette (refined parameters),
3. forced collision in cell 21,
4. DXTRAN with DXCPN probabilities, and
5. ring detector.

Figure 23 shows the results of the first run. Note that, as expected, the tallies and FOMs have decreased substantially. The geometry splitting could probably be improved somewhat to keep the “tracks entering” roughly constant.

TABLE II. Exponential Biasing Parameter

k	Cumulative Probability	Theta	Weight
.01	0	0	0.990
	0.25	60	0.995
	0.50	90	1.000
	0.75	120	1.005
	1.00	180	1.010
1	0	0	0.432
	0.25	42	0.552
	0.50	64	0.762
	0.75	93	1.230
	1.00	180	3.195
2	0	0	0.245 ^a
	0.25	31	0.325
	0.50	48	0.482
	0.75	70	0.931
	1.00	180	13.40
3.5	0	0	0.143
	0.25	23	0.190
	0.50	37	0.285
	0.75	53	0.569
	1.00	180	156.5

^ak = 2 was chosen because the weight is approximately 2 at 90°, which is eight times the weight at 0°; this does not seem unreasonable.

Before worrying about optimizing the geometry splitting, I shall discuss the effect of source energy biasing because first, geometry splitting optimization has already been illustrated, and second, the source energy biasing will increase the energy spectrum of the tracks, making the average track penetrate better. Tracks with longer free paths will need less splitting to keep the tracks entering approximately constant. In short, the “tracks entering” column in Fig. 23 can be expected to improve because of source energy biasing.

D. Source Energy Bias

MCNP allows biasing the source in the energy domain as well as in the angular domain. In biasing, the SB card is used with the SI and SP cards. The SI card supplies energy ranges, the SP card supplies analog probabilities, and the SB card supplies the actual probabilities used to sample the energy ranges. Before attempting a long run, look at the source bias information in the MCNP output and check that the weight multiplier is not unreasonable. Figure 24 is an example of the source bias information from the run described next.

Recall that the natural source is 95% at 2 MeV and 5% at 14 MeV. It is a good guess (based on experience) that the 14-MeV source neutrons are much more important than the 2-MeV source neutrons; therefore, I biased the source to get 10% at 2 MeV and 90% at 14 MeV. The “weight multiplier” column in Fig. 24 shows that the ratio of weights is 171; that is, the source energy biasing assumes that 14-MeV neutrons are 171 times as important as 2-MeV neutrons. This seems too high until one considers that 180 cm of concrete must be penetrated. The 14-MeV neutrons can probably penetrate 171 times better. In any case, thousands of neutrons are run, which means that there will be hundreds of 2-MeV source neutrons. Thus the statistics can indicate whether 171 is much too large because 2-MeV source neutrons are not precluded by the source biasing.

Figure 25 shows the results of the source energy biasing. All FOMs increased by a factor of 4 and, as predicted, the “tracks entering” column has improved substantially. Source energy biasing has definitely improved things, but could the same improvement be obtained using the energy splitting and roulette scheme that was successful earlier?

E. Energy Roulette (Without Source Energy Bias) Applied to the Sample Problem

Figure 26 shows the results of removing the source energy bias and inserting the energy roulette game:

50% survival crossing 5-MeV, 1-MeV, 0.3-MeV, 0.1-MeV and 0.03-MeV energy bounds.

The FOMs are a factor of 2 better than the reference case (Fig. 23) that had no biasing in the energy domain, but a factor of 2 worse than the source energy biasing. The “tracks entering” column is flat deep into the concrete cylinder but decreasing very fast at the source end. This decrease is probably because the 2-MeV particles fail to survive the energy roulette game. Indeed, a look at the creation and loss ledger (Fig. 27) tends to confirm that energy roulette is killing a lot of tracks. The energy splitting and Russian roulette are the “ENERGY IMPORT” entries.

CELL PROGR	PROBL	TRACKS ENTERING	POPULATION	COLLISIONS	COLLISIONS * WEIGHT (PER HISTORY)	NUMBER WEIGHTED ENERGY	FLUX WEIGHTED ENERGY	AVERAGE TRACK WEIGHT (RELATIVE)	AVERAGE TRACK MFP (CM)	NOTE: HAS DECREASED
2	2	5914	5720	11445	1.9890E+00	2.2985E+00	6.1297E+00	7.7324E-01	6.9710E+00	
3	3	5307	4923	11491	1.0608E+00	1.0972E+00	3.9329E+00	8.1038E-01	5.8903E+00	
4	4	5111	4763	11787	5.9832E-01	8.5958E-01	3.2519E+00	8.8653E-01	5.5618E+00	
5	5	5180	4810	11538	2.7965E-01	7.2047E-01	2.9029E+00	9.1888E-01	5.4167E+00	
6	6	5015	4616	11211	1.3685E-01	7.0215E-01	2.7985E+00	9.3529E-01	5.3996E+00	
7	7	4695	4312	10524	6.2767E-02	7.2576E-01	2.7575E+00	9.1509E-01	5.4285E+00	
8	8	4242	3945	9629	2.9178E-02	7.1694E-01	2.6206E+00	9.2397E-01	5.3921E+00	
9	9	4161	3854	9329	1.4144E-02	6.1629E-01	2.4115E+00	9.8567E-01	5.2563E+00	
10	10	4285	3955	9734	6.4125E-03	6.9663E-01	2.4682E+00	9.3585E-01	5.3448E+00	
11	11	4384	4053	9845	3.0105E-03	6.9835E-01	2.3887E+00	9.2738E-01	5.3195E+00	
12	12	4273	3992	9556	1.3470E-03	6.7214E-01	2.3123E+00	9.2956E-01	5.2919E+00	
13	13	4117	3814	8807	5.9640E-04	6.1880E-01	2.3277E+00	9.3717E-01	5.2995E+00	
14	14	4147	3828	9325	2.7289E-04	7.4179E-01	2.4115E+00	8.9202E-01	5.4420E+00	
15	15	4261	3980	9609	1.3223E-04	7.3805E-01	2.3203E+00	8.9575E-01	5.3573E+00	
16	16	4505	4207	9857	5.8674E-05	7.5736E-01	2.4096E+00	8.7379E-01	5.5164E+00	
17	17	4715	4376	10409	2.7660E-05	7.9721E-01	2.4079E+00	8.5441E-01	5.5688E+00	
18	18	4973	4612	11199	1.4528E-05	7.1284E-01	2.2599E+00	9.0298E-01	5.4450E+00	
19	19	4813	4667	10456	5.8531E-06	7.3157E-01	2.3271E+00	8.8620E-01	5.5518E+00	
20	20	5247	17752	0	0.	1.6527E+00	3.7587E+00	3.1599E-01	1.0000+123	
21	21	14447	28900	14780	5.7952E-11	1.7306E+00	4.2168E+00	3.9238E-04	7.2168E+02	
22	22	1218	1218	0	0.	2.9313E-01	1.3919E+00	2.3560E-05	1.0000+123	
TOTAL		105010	126297	200531	4.1826E+00					

IF ANYTHING, THE RESULTS ARE WORSE

TALLY 1			TALLY 4			TALLY 5				
NPS	MEAN	ERROR	FOM	MEAN	ERROR	FOM	MEAN	ERRDR	FOM	
1000	6.76998E-07	.2279	35	1.08405E-13	.2017	45	6.41533E-17	.2303	34	
2000	7.76445E-07	.1899	26	1.17538E-13	.1684	33	7.32270E-17	.1813	29	
3000	6.57440E-07	.1608	27	1.01848E-13	.1424	34	6.21477E-17	.1533	29	
4000	6.44592E-07	.1331	30	9.99931E-14	.1212	36	6.17369E-17	.1294	31	
5000	6.53824E-07	.1144	32	1.02744E-13	.1045	38	6.25061E-17	.1115	33	
5404	6.78768E-07	.1073	33	1.05245E-13	.0984	39	6.43094E-17	.1042	35	
			38 = NO BIAS				44 = NO BIAS	41 = NO BIAS		

DUMP NO. 2 ON FILE RUNTPG			NPS = 5404			CTM = 2.59				

Fig. 22. Exponential source biasing, K = 2.0.

95% AT 2 MeV 5% AT 14 MeV

CELL PROGR PROBL	TRACKS ENTERING	POPULATION	COLLISIONS	COLLISIONS * WEIGHT (PER HISTORY)	NUMBER WEIGHTED ENERGY	FLUX WEIGHTED ENERGY	AVERAGE TRACK WEIGHT (RELATIVE)	AVERAGE TRACK MFP (CM)
2 2	36626	35147	84028	2.5392E+00	8.1404E-01	1.6748E+00	1.0000E+00	5.0804E+00
3 3	20612	17717	89215	1.2254E+00	4.1376E-01	1.0791E+00	1.0000E+00	4.1250E+00
4 4	16863	14731	71948	4.7060E-01	3.3049E-01	9.6776E-01	1.0000E+00	3.8814E+00
5 5	12689	11113	52606	1.5640E-01	3.1602E-01	1.0160E+00	1.0000E+00	3.8749E+00
6 6	8232	7213	33982	5.0516E-02	3.1378E-01	1.1137E+00	1.0000E+00	3.9250E+00
7 7	5345	4665	22071	1.6405E-02	3.3660E-01	1.2637E+00	1.0000E+00	4.0813E+00
8 8	3499	3078	13604	5.0558E-03	3.8861E-01	1.5567E+00	1.0000E+00	4.3308E+00
9 9	2704	2388	10299	1.7802E-03	4.6442E-01	1.8798E+00	1.0000E+00	4.6472E+00
10 10	2126	1870	7936	6.3804E-04	5.6864E-01	2.1439E+00	1.0000E+00	5.0175E+00
11 11	1940	1687	7020	2.6251E-04	6.4275E-01	2.3902E+00	1.0000E+00	5.3084E+00
12 12	1847	1603	6787	1.1804E-04	6.8158E-01	2.4418E+00	1.0000E+00	5.4103E+00
13 13	1935	1649	6835	5.5293E-05	6.8520E-01	2.4479E+00	1.0000E+00	5.4328E+00
14 14	1921	1651	6909	2.5996E-05	6.7867E-01	2.3340E+00	1.0000E+00	5.3967E+00
15 15	1864	1622	6958	1.2177E-05	6.7540E-01	2.3111E+00	1.0000E+00	5.3200E+00
16 16	1827	1610	6515	5.1826E-06	6.8789E-01	2.3831E+00	1.0000E+00	5.4192E+00
17 17	1752	1542	6225	2.2509E-06	6.9864E-01	2.3035E+00	1.0000E+00	5.3890E+00
18 18	1719	1508	6112	1.0044E-06	6.4792E-01	2.2378E+00	9.9959E-01	5.3291E+00
19 19	1460	1379	5244	3.9020E-07	7.2496E-01	2.3171E+00	9.9710E-01	5.5252E+00
20 20	2987	10250	0	0.	1.5228E+00	3.7671E+00	2.1540E-01	1.0000+123
21 21	9646	19293	9982	4.0126E-12	1.9111E+00	4.6916E+00	2.4317E-04	7.4538E+02
22 22	962	962	0	0.	4.8276E-01	1.7833E+00	7.7522E-06	1.0000+123
TOTAL	138556	142678	454276	4.4665E+00				

MIGHT HELP TO
INCREASE SPLITTING

INFLUENCE OF
FORCED COLLISION

NPS	TALLY 1			FOM	TALLY 4			FOM	TALLY 5			FOM
	MEAN	ERROR			MEAN	ERROR			MEAN	ERROR		
2000	4.20276E-08	.7812		5	6.75611E-15	.8612		4	3.79689E-18	.8929		4
4000	3.33748E-08	.6050		4	5.80450E-15	.6311		4	3.40807E-18	.6406		4
6000	2.47221E-08	.5491		4	4.27827E-15	.5756		3	2.58330E-18	.5725		3
8000	2.00867E-08	.5094		3	3.69877E-15	.5063		3	2.36517E-18	.4839		4
10000	2.07666E-08	.4301		4	4.19567E-15	.4050		4	2.51507E-18	.4027		4
12000	3.52290E-08	.3672		4	6.77026E-15	.3363		5	4.08518E-18	.3521		4
14000	4.67954E-08	.3164		4	8.74776E-15	.3154		4	5.06476E-18	.3118		5
16000	4.68175E-08	.2868		5	8.55125E-15	.2883		5	4.90277E-18	.2871		5
18000	4.54612E-08	.2694		5	8.38284E-15	.2704		5	4.81680E-18	.2686		5
20000	4.25220E-08	.2607		5	7.73913E-15	.2640		4	4.46717E-18	.2614		5
22000	4.95566E-08	.2771		4	8.53243E-15	.2606		4	4.88221E-18	.2581		4
24000	4.84141E-08	.2672		4	8.39374E-15	.2522		4	4.76392E-18	.2499		4
26000	4.54506E-08	.2633		3	7.89398E-15	.2483		4	4.49672E-18	.2454		4
28000	4.49413E-08	.2505		4	7.80158E-15	.2366		4	4.45104E-18	.2334		4
30000	4.68896E-08	.2341		4	8.07256E-15	.2230		4	4.62160E-18	.2201		4
32000	4.39590E-08	.2342		4	7.56834E-15	.2230		4	4.33278E-18	.2201		4
33092	4.43014E-08	.2265		4	7.57040E-15	.2166		4	4.34913E-18	.2134		4

DUMP NO. 2 ON FILE RUNTPE NPS = 33092 CTM = 4.60

Fig. 23. New source (angle bias and energy roulette removed).

SOURCE = 1

SOURCE COEFFICIENTS

1	0.
2	1.0000E-06
3	0.
4	2.0000E+00
5	1.0000E+00

BIASED SOURCE DISTRIBUTION 0				SP card	SB card	
SOURCE ENTRY	SOURCE VALUE	CUMULATIVE PROBABILITY	BIASED CUMULATIVE	PROBABILITY DENSITY	BIASED PROBABILITY	WEIGHT MULTIPLIER
1	2.0000E+00	9.50000E-01	1.00000E-01	9.50000E-01	1.00000E-01	9.50000E+00
2	1.4000E+01	1.00000E+00	1.00000E+00	5.00000E-02	9.00000E-01	5.55556E-02

AVERAGE VALUE USING BIN MIDPOINTS = 2.6000E+00

Fig. 24. SI, SP, and SB cards in source energy bias.

NATURAL 95% 2MeV 10% 2MeV
 5% 14MeV **BIASED** → 90% 14 MeV

CELL PROGR PROBL	TRACKS ENTERING	POPULATION	COLLISIONS	COLLISIONS + WEIGHT (PER HISTORY)	NUMBER WEIGHTED ENERGY	FLUX WEIGHTED ENERGY	AVERAGE TRACK WEIGHT (RELATIVE)	AVERAGE TRACK MFP (CM)
2	2	6972	6719	11236	2.4159E+00	8.4842E-01	9.9753E-01	5.1519E+00
3	3	4563	3961	15126	1.1709E+00	4.3988E-01	1.1247E+00	4.1335E+00
4	4	5203	4515	18181	4.4346E-01	3.5671E-01	1.0511E+00	5.3181E-01
5	5	5812	5042	20223	1.4352E-01	3.7649E-01	1.1059E+00	3.5288E-01
6	6	5698	4915	20329	4.1596E-02	3.5477E-01	1.2067E+00	2.1776E-01
7	7	5384	4627	19703	1.3995E-02	4.1701E-01	1.4003E+00	1.5920E-01
8	8	5329	4595	18889	6.3198E-03	3.6196E-01	1.3787E+00	1.3716E-01
9	9	5420	4702	19148	1.8645E-03	4.0415E-01	1.7327E+00	9.2617E-02
10	10	5645	4879	20119	7.4253E-04	4.6754E-01	1.9855E+00	7.6064E-02
11	11	5920	5134	21337	3.0860E-04	5.6113E-01	2.1422E+00	6.7175E-02
12	12	6078	5264	21968	1.1915E-04	6.4761E-01	2.3362E+00	5.7361E-02
13	13	6288	5463	22861	5.3917E-05	6.6897E-01	2.3569E+00	5.5556E-02
14	14	6174	5435	22266	2.4425E-05	6.8243E-01	2.3400E+00	5.5556E-02
15	15	6340	5532	23227	1.1851E-05	6.8723E-01	2.2842E+00	5.5556E-02
16	16	6683	5821	24654	5.7176E-06	6.6909E-01	2.2022E+00	5.5556E-02
17	17	6938	6049	25412	2.6788E-06	6.4062E-01	2.1177E+00	5.5556E-02
18	18	6635	5848	24702	1.1836E-06	6.4581E-01	2.0951E+00	5.5556E-02
19	19	5798	5450	20798	4.5270E-07	6.9464E-01	2.2024E+00	5.5530E-02
20	20	7473	22973	0	0.	1.2085E+00	3.2355E+00	2.0560E-02
21	21	20687	41375	21355	4.6036E-12	1.7734E+00	4.2512E+00	2.4781E-05
22	22	1928	1928	0	0.	6.3728E-01	2.0664E+00	9.6952E-07
TOTAL		136968	160227	391534	4.2388E+00			

NPS	TALLY 1		FOM	TALLY 4		FOM	TALLY 5		FOM
	MEAN	ERROR		MEAN	ERROR		MEAN	ERROR	
1000	3.85940E-08	.2906	17	6.20273E-15	.2767	19	3.79043E-18	.2697	20
2000	4.75214E-08	.2030	17	8.09356E-15	.2009	17	4.94164E-18	.1957	18
3000	4.14782E-08	.1799	15	8.04785E-15	.1792	15	4.51650E-18	.1745	16
4000	4.48775E-08	.1479	16	8.08531E-15	.1480	16	4.74614E-18	.1428	17
5000	4.48569E-08	.1303	16	8.12581E-15	.1303	17	4.74559E-18	.1258	18
6000	4.81852E-08	.1195	16	8.53562E-15	.1169	16	5.06492E-18	.1139	17
6306	4.90487E-08	.1149	16	8.60624E-15	.1126	17	5.10226E-18	.1099	17

***** 4 NO E BIAS ***** 4 NO ENERGY BIAS ***** 4 NO E BIAS *****
 DUMP NO. 2 ON FILE RUNTPF NPS = 6306 CTM = 4.63

CONCLUSION: SOURCE ENERGY BIAS HERE QUITE USEFUL

WEIGHT (2MeV) = 9.5
 WEIGHT (14 MeV) = 5.556E - 2

**COMPARE TO ENERGY
 ROULETTE ON NEXT RUN**

Fig. 25. Energy bias on source.

50% SURVIVAL AS CROSS ENERGY BOUNDS 5 1 0.3 0.1 0.03

CELL PROGR PROBL	TRACKS ENTERING	POPULATION	COLLISIONS	COLLISIONS * WEIGHT (PER HISTORY)	NUMBER WEIGHTED ENERGY	FLUX WEIGHTED ENERGY	AVERAGE TRACK WEIGHT (RELATIVE)	AVERAGE TRACK MFP (CM)
2 2	70107	68555	111894	2.6091E+00	7.8547E-01	1.6404E+00	1.3098E+00	5.0400E+00
3 3	28187	25777	86177	1.2351E+00	4.2534E-01	1.0934E+00	1.7163E+00	4.1322E+00
4 4	19828	18176	60187	4.6799E-01	3.3841E-01	9.9897E-01	1.9583E+00	3.9106E+00
5 5	13820	12737	41740	1.6086E-01	3.1246E-01	1.0617E+00	2.1207E+00	3.9001E+00
6 6	8586	7917	25110	5.0656E-02	3.4457E-01	1.2451E+00	2.1743E+00	4.0577E+00
7 7	5552	5098	15603	1.6388E-02	3.9613E-01	1.4552E+00	2.2459E+00	4.2423E+00
8 8	3870	3551	10631	5.4346E-03	4.8289E-01	1.7392E+00	2.2241E+00	4.5756E+00
9 9	3051	2810	7946	2.3048E-03	4.1794E-01	1.7727E+00	2.5434E+00	4.5869E+00
10 10	2479	2288	6335	8.1435E-04	5.6787E-01	2.1160E+00	2.3964E+00	5.0126E+00
11 11	2262	2091	5371	3.4185E-04	5.9145E-01	2.2002E+00	2.4426E+00	5.1905E+00
12 12	2137	1991	4679	1.3379E-04	7.2614E-01	2.3382E+00	2.3497E+00	5.4811E+00
13 13	2065	1909	4585	5.8148E-05	7.7816E-01	2.3630E+00	2.3155E+00	5.5358E+00
14 14	1941	1806	4342	2.8205E-05	6.1960E-01	2.1829E+00	2.5192E+00	5.2813E+00
15 15	1864	1729	4389	1.3275E-05	6.9134E-01	2.0983E+00	2.5261E+00	5.3021E+00
16 16	1879	1746	4490	6.8583E-06	6.1553E-01	1.9085E+00	2.7108E+00	5.1032E+00
17 17	1844	1702	4486	2.8800E-06	6.6752E-01	1.9462E+00	2.6280E+00	5.2474E+00
18 18	1870	1706	4409	1.4005E-06	6.0413E-01	1.9480E+00	2.7121E+00	5.1846E+00
19 19	1736	1690	3923	5.0556E-07	7.2824E-01	2.1497E+00	2.5339E+00	5.4375E+00
20 20	2709	10111	0	0.	9.3521E-01	2.7747E+00	7.2627E-01	1.0000+123
21 21	8535	17070	8755	5.4317E-12	1.7017E+00	4.0791E+00	7.6034E-04	7.3132E+02
22 22	747	747	0	0.	1.2796E+00	2.0507E+00	2.5020E-05	1.0000+123
TOTAL	185069	191207	415052	4.5493E+00				

LOST TO E
ROULETTE PROBABLY
↓
CHECK CREATION
AND LOSS PAGE

NPS	TALLY 1			FOM	TALLY 4			FOM	TALLY 5		
	MEAN	ERROR			MEAN	ERROR			MEAN	ERROR	FOM
4000	5.62428E-08	.5925		9	1.10868E-14	.5061	12	6.85957E-18	.5109	12	
8000	6.21143E-08	.4683		7	1.39254E-14	.3725	12	8.49671E-18	.3930	10	
12000	6.83978E-08	.3618		8	1.28214E-14	.3109	11	7.50953E-18	.3265	10	
16000	5.96421E-08	.3216		8	1.14008E-14	.2748	11	6.49283E-18	.2912	10	
20000	6.51427E-08	.2646		9	1.22680E-14	.2305	13	7.27391E-18	.2412	11	
24000	6.64407E-08	.2498		9	1.21877E-14	.2257	11	7.24270E-18	.2323	10	
28000	6.93985E-08	.2315		9	1.17701E-14	.2106	11	6.89511E-18	.2172	10	
32000	6.48955E-08	.2195		9	1.08231E-14	.2021	10	6.29969E-18	.2092	10	
36000	6.16679E-08	.2091		9	1.04173E-14	.1921	10	5.95547E-18	.1998	9	
40000	6.56990E-08	.1862	10	1.07598E-14	.1740	11	6.19549E-18	.1798	10		
44000	6.09625E-08	.1830	9	1.00179E-14	.1705	11	5.75220E-18	.1764	10		
48000	6.10327E-08	.1752	9	9.84176E-15	.1628	11	5.63330E-18	.1686	10		
52000	6.00462E-08	.1675	9	9.56935E-15	.1566	11	5.51862E-18	.1624	10		
56000	6.18936E-08	.1604	10	9.46712E-15	.1501	11	5.42811E-18	.1558	10		
60000	6.67085E-08	.1566	9	1.02460E-14	.1452	11	6.18120E-18	.1536	10		
64000	6.34663E-08	.1550	9	9.75654E-15	.1435	10	5.89703E-18	.1517	9		
66475	6.21818E-08	.1529	9	9.79947E-15	.1405	10	5.93803E-18	.1482	9		

***** ENERGY SOURCE BIAS ***** ENERGY BIAS ENERGY BIAS *****
 DUMP NO. 2 ON FILE RUNTPG NPS = 66475 CTM = 4.61

10 TIMES AS MANY PARTICLES STARTED
AS WITH ENERGY SOURCE BIASING

Fig. 26. No energy source bias; energy roulette used.

RUN TERMINATED 19 SECONDS BEFORE JOB TIME LIMIT.

SAMPLE PROBLEM FOR MFE TALKS

S 09/19/83 11:13:02

NO PARTICLES UPSCATTERED LEDGER OF NET NEUTRON CREATION AND LOSS (FOR ACCOUNTING ONLY)

	TRACKS	WEIGHT (PER SOURCE PARTICLE)	ENERGY (PER SOURCE PARTICLE)
SOURCE	66475	1.0000E+00	2.5991E+00
SCATTERING	0	0.	0.
FISSION	0	0.	0.
(N,XN)	67	3.6737E-04	9.1998E-04
FORCED COLLISION	8535	0.	0.
WEIGHT CUTOFF	0	0.	0.
WEIGHT WINDOW	0	0.	0.
CELL IMPORTANCE	49918	1.1656E-01	1.0066E-01
ENERGY IMPORT.	0	4.6479E-01	1.5012E-01
DXTRAN	9343	3.0923E-10	1.2561E-09
EXP. TRANSFORM	0	0.	0.
TOTAL	134338	1.5817E+00	2.8508E+00

LARGE NUMBER LOST TO ENERGY ROULETTE

	TRACKS	WEIGHT (PER SOURCE PARTICLE)	ENERGY (PER SOURCE PARTICLE)
ESCAPE	62929	7.6327E-01	1.6367E+00
SCATTERING	0	0.	8.6664E-01
CAPTURE	2514	8.6574E-03	9.5842E-02
ENERGY CUTOFF	5590	2.3566E-01	1.2582E-03
TIME CUTOFF	0	0.	0.
WEIGHT CUTOFF	0	0.	0.
WEIGHT WINDOW	0	0.	0.
CELL IMPORTANCE	14468	1.1712E-01	1.0112E-01
ENERGY IMPORT.	48832	4.5701E-01	1.4924E-01
DXTRAN	5	7.8099E-10	8.0133E-10
EXP. TRANSFORM	0	0.	0.
DEAD FISSION	0	0.	0.
TOTAL	134338	1.5817E+00	2.8508E+00

PREDICTED AVG OF SRC FUNCTION ZERO 2.6000E+00
 TRACKS PER NEUTRON STARTED 2.0209E+00
 COLLISIONS PER NEUTRON STARTED 6.2437E+00
 TOTAL COLLISIONS 415052
 NET MULTIPLICATION 1.0004E+00 .0001

AVERAGE LIFETIME, SHAKES
 ESCAPE 5.2613E-01
 CAPTURE 6.7963E-01
 CAPTURE OR ESCAPE 5.2785E-01
 ANY TERMINATION 2.5120E+00

CUTOFFS
 TCO 1.0000+123
 ECO 1.0000E-02
 WC1 0.
 WC2 0.

COMPUTER TIME SO FAR IN THIS RUN 4.66 MINUTES
 COMPUTER TIME IN MCRUN (4CO) 4.61 MINUTES
 SOURCE PARTICLES PER MINUTE 1.4420E+04
 FIELD LENGTH 371584 = 1325600B
 RANDOM NUMBERS GENERATED 4653934
 LAST STARTING RANDOM NUMBER 3305404155025121B
 NEXT STARTING RANDOM NUMBER 7246405510430155B

TOTAL NEUTRONS BANKED 61820
 PER SOURCE PARTICLE 9.2997E-01
 TOTAL PHOTONS BANKED 0
 PER SOURCE PARTICLE 0.
 MAXIMUM NUMBER EVER IN BANK 44
 BANK OVERFLOWS TO DISK 0

Fig. 27. Creation and loss ledger—energy roulette, no source biasing.

F. Source Energy Biasing and Energy Roulette Applied to the Sample Problem

Both source energy biasing and energy roulette individually improved the FOMs. The natural temptation at this point is to try both techniques and hope for improvement. Before trying both techniques, a suspicious person might wonder whether *two* energy biasing techniques would be too much of a good thing. Would the calculation be overbiased? Fortunately, for reasons explained below, the techniques work well together.

Figure 28 gives the results of using both source energy biasing and energy roulette. First, note that the "tracks entering" column looks very nice. Second, note that the FOMs are

1. a factor of 4 better than energy roulette alone,
2. a factor of 2 better than source energy bias alone, and
3. a factor of 8 better than with neither energy roulette nor source energy bias.

Hindsight, aided by elementary arithmetic ($4 \cdot 2 = 8$) indicates that the two techniques operate essentially independently. Although both are energy biasing, they are biasing different things. Source energy biasing is applied only at the source and supplies the right initial spectrum; thereafter it does nothing to keep the right spectrum after collisions. In contrast, the energy roulette technique does nothing to alter the effects of the initial spectrum. That is, if N_1 14-MeV source tracks produce a track distribution $n_1(\vec{r}, \vec{v}, t)$, biasing the source to instead produce N_2 14-MeV source tracks will produce a track distribution $n_2(\vec{r}, \vec{v}, t) = (N_2/N_1)n_1(\vec{r}, \vec{v}, t)$. The energy roulette game takes no account of the source energy biasing. Synergism can be viewed as follows: the source energy bias produces good initial track distribution on which the energy roulette works to produce a good subsequent track distribution. However, if the initial track distribution is not good, the subsequent track distribution cannot be good because the energy roulette game is independent of the initial track distribution and therefore cannot "correct" it. Energy splitting/Russian roulette thus contrasts with the next energy-biasing technique considered, the space-energy-dependent weight window. The weight window, if set properly, will correct poor track distributions and if set poorly, will destroy good track distributions.

XIII. THE WEIGHT WINDOW TECHNIQUE

The weight window (Fig. 29) is a space-energy-dependent splitting and Russian roulette technique. For each space-energy phase-space cell, the user supplies a lower weight bound and an upper weight bound. These weight bounds define a window of acceptable weights. If a particle is below the lower weight bound, Russian

roulette is played and the particle's weight is either increased to be within the window, or the particle is terminated. If a particle is above the upper weight bound, the particle is split so that all the split particles are within the window. No action is taken for particles within the window.

Figure 30 is a more detailed picture of the weight window. Three important weights define the weight window in a space-energy cell,

1. W_L , the lower weight bound,
2. W_S , the survival weight for particles playing roulette, and
3. W_U , the upper weight bound.

The user specifies (WFN cards) W_L for each space-energy cell, and W_S and W_U are calculated using two problem-wide constants, C_S and C_U (WDWN card), as $W_S = C_S W_L$ and $W_U = C_U W_L$. Thus all cells have an upper weight bound C_U times the lower weight bound and a survival weight C_S times the lower weight bound.

A. Weight Window Compared to Geometry Splitting

Although both weight window and geometry splitting employ splitting and Russian roulette, there are some important differences:

1. the weight window is space-energy dependent, whereas geometry splitting is only space dependent;
2. the weight window discriminates on particle weight before deciding appropriate action, whereas geometry splitting is done regardless of particle weight;
3. the weight window works with absolute weight bounds, whereas geometry splitting is done on the *ratio* of the importances across a surface;
4. the weight window can be applied at surfaces, collision sites, or both, whereas geometry splitting is applied only at surfaces; and
5. the weight window can control weight fluctuations introduced by other biasing techniques by requiring all particles in a cell to have weight $W_L < W < W_U$, whereas the geometry splitting will preserve any weight fluctuations because it is weight independent.

B. Special Weight Window Features Described in MCNP Manual¹

1. There is a maximum split/roulette feature that limits the amount of splitting/rouletting that can occur at any particular weight window game.
2. The window is always adjusted to be at least a factor of 2 wide, that is $W_U/W_L \geq 2$.
3. A spatial weight window (only one energy range) may be specified inversely proportional to

CELL PROGR	PROBL	TRACKS ENTERING	POPULATION	COLLISIONS	COLLISIONS * WEIGHT (PER HISTORY)	NUMBER WEIGHTED ENERGY	FLUX WEIGHTED ENERGY	AVERAGE TRACK WEIGHT (RELATIVE)	AVERAGE TRACK MFP (CM)
2	2	17683	17421	18401	2.9228E+00	6.5198E-01	1.5652E+00	1.4126E+00	4.9220E+00
3	3	8189	7706	16529	1.2165E+00	4.0135E-01	1.1114E+00	1.3999E+00	4.1031E+00
4	4	8169	7614	16990	4.9640E-01	3.0337E-01	9.8723E-01	1.1273E+00	3.8762E+00
5	5	8536	7961	18531	1.4888E-01	3.0433E-01	1.1073E+00	7.2806E-01	3.9825E+00
6	6	7933	7319	16656	3.6534E-02	4.6654E-01	1.3970E+00	4.2323E-01	4.2507E+00
7	7	7628	7053	16376	1.3413E-02	3.0623E-01	1.4438E+00	3.3037E-01	4.2524E+00
8	8	7469	6918	16581	5.5635E-03	2.5863E-01	1.5428E+00	2.7380E-01	4.3058E+00
9	9	7545	7028	16253	1.2710E-03	7.7427E-01	2.3836E+00	1.6293E-01	5.2930E+00
10	10	7743	7203	16785	5.7509E-04	7.5529E-01	2.5027E+00	1.4951E-01	5.4140E+00
11	11	8053	7458	17529	2.8978E-04	7.9740E-01	2.3184E+00	1.5977E-01	5.3391E+00
12	12	8444	7789	18993	1.5350E-04	6.1156E-01	2.0427E+00	1.7034E-01	5.0493E+00
13	13	8326	7719	19073	9.0588E-05	3.9260E-01	1.6872E+00	2.0404E-01	4.6376E+00
14	14	8054	7500	18292	4.1931E-05	3.6699E-01	1.7155E+00	1.8709E-01	4.6382E+00
15	15	7951	7353	18213	1.2188E-05	6.9409E-01	2.2246E+00	1.4018E-01	5.3930E+00
16	16	7914	7356	18333	5.5212E-06	6.9344E-01	2.1793E+00	1.4163E-01	5.3620E+00
17	17	8124	7558	18452	2.7658E-06	6.3633E-01	2.0456E+00	1.5086E-01	5.2695E+00
18	18	7959	7429	18246	1.1762E-06	6.6921E-01	2.0945E+00	1.4122E-01	5.3503E+00
19	19	7487	7257	16836	4.7207E-07	6.8370E-01	2.1757E+00	1.3770E-01	5.4548E+00
20	20	9186	33133	0	0.	1.1969E+00	3.2996E+00	4.3458E-02	1.0000+123
21	21	27603	55209	28270	4.7499E-12	1.7495E+00	4.1883E+00	5.3933E-05	7.4440E+02
22	22	2344	2344	0	0.	8.8156E-01	2.4404E+00	2.0311E-06	1.0000+123
TOTAL		192340	234328	345339	4.8425E+00				

NPS	TALLY 1			TALLY 4			TALLY 5		
	MEAN	ERROR	FOM	MEAN	ERROR	FOM	MEAN	ERROR	FOM
1000	6.75738E-08	.3135	33	1.02821E-14	.2841	40	6.11613E-18	.2781	42
2000	5.30839E-08	.2317	35	8.19119E-15	.2050	45	4.78299E-18	.2057	44
3000	4.74756E-08	.1977	33	7.70589E-15	.1733	43	4.64642E-18	.1780	41
4000	4.16499E-08	.1768	32	7.08741E-15	.1546	42	4.18273E-18	.1585	40
5000	4.18353E-08	.1530	35	7.13209E-15	.1344	45	4.18036E-18	.1392	42
6000	4.47058E-08	.1361	35	7.84299E-15	.1191	46	4.48464E-18	.1231	43
7000	4.90518E-08	.1218	36	8.58856E-15	.1082	46	4.92879E-18	.1119	43
8000	5.06288E-08	.1114	36	8.89479E-15	.0982	47	5.13099E-18	.1017	44
9000	5.26031E-08	.1032	37	9.16675E-15	.0917	47	5.26253E-18	.0950	43
10000	5.16829E-08	.0979	37	9.00032E-15	.0867	47	5.15435E-18	.0898	44
11000	5.17916E-08	.0947	36	8.90241E-15	.0834	46	5.13525E-18	.0867	43
12000	5.27634E-08	.0917	35	9.07606E-15	.0810	45	5.35139E-18	.0850	40
13000	5.40505E-08	.0874	35	9.17604E-15	.0774	45	5.40450E-18	.0809	41
14000	5.17889E-08	.0861	35	8.78389E-15	.0762	44	5.17840E-18	.0799	40
15000	5.19164E-08	.0831	34	8.94873E-15	.0739	44	5.28099E-18	.0779	39
16000	5.12984E-08	.0805	35	8.78145E-15	.0721	43	5.20501E-18	.0758	39
16957	5.04281E-08	.0803	33	8.81392E-15	.0759	37	5.14446E-18	.0755	38

 16 SOURCE ENERGY BIASING WITH 17 NO ENERGY ROULETTE 17

 DUMP NO. 2 ON FILE RUNTPH NPS = 16957 CTM = 4.61

CONCLUSION - GOOD IDEA TO USE BOTH

COMPARE WITH 6306 FOR SOURCE BIASING IN ENERGY WITHOUT ENERGY ROULETTE

Fig. 28. Source biasing and energy roulette.

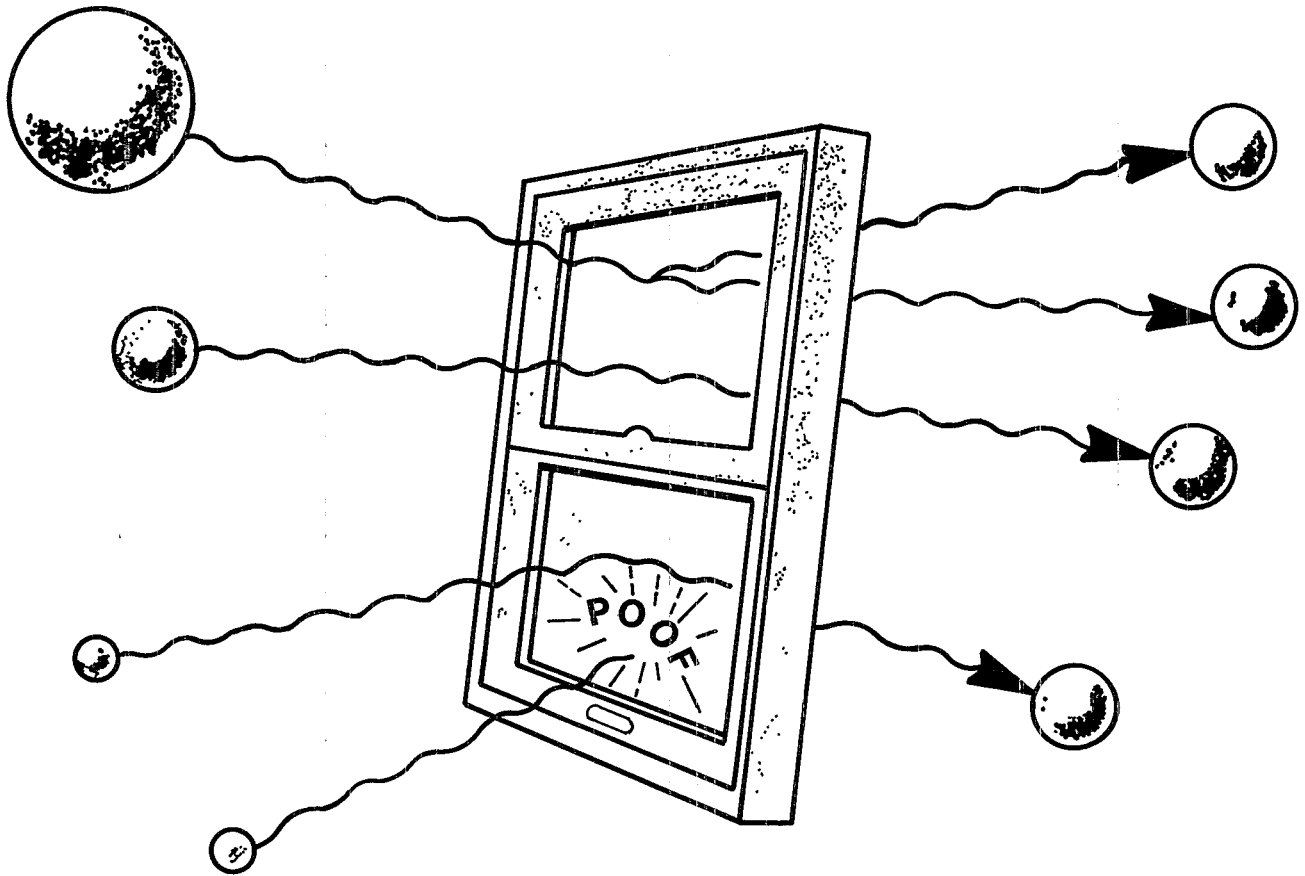


Fig. 29. The weight window. Tracks entering a phase-space cell with weight above the window's upper bound are split into several tracks within the window. Those with weights below the window play Russian Roulette. Therefore, particles passing through the window have weights within the window bounds.

previously optimized cell importances from the geometry-splitting technique.

$$W_L = 0.5/\text{cell importances}$$

$$W_S = 3.0 \cdot W_L$$

$$W_U = 5.0 \cdot W_L$$

lower weight bound
survival weight
upper weight bound

C. Specifying the Weight Windows for the Sample Problem

The weight window parameters should be such that the weight windows are inversely proportional to the space-energy importance. Thus one must either guess what the importance function looks like or use information from experience. The geometry-splitting optimization has already provided a spatial importance function that can be used (see item 3 in Sec. XIII.B) to obtain a space-only weight window. If the cell importances were not available, one could either pick window parameters that flattened the track distribution (in the same iterative procedure used for geometry splitting) or one could use the weight window generator described later.

The weight windows are chosen according to available cell importances (except for cells 20-22).

Furthermore (see item 1 in Sec. XIII.B), no particle (in any given game) will be split more than five for one, nor rouletted harsher than one in five. The weight window game was turned off in cells 20-22 because that part of the problem is too angle dependent for the weight window to be effective. The weight window was applied both at collisions and surface crossings.

D. Spatial Weight Window Results

The source energy bias and energy roulette were removed for this run. The following techniques were used:

1. energy cutoff,
2. forced collision in cell 21,
3. DXTRAN with DXCPN probabilities,

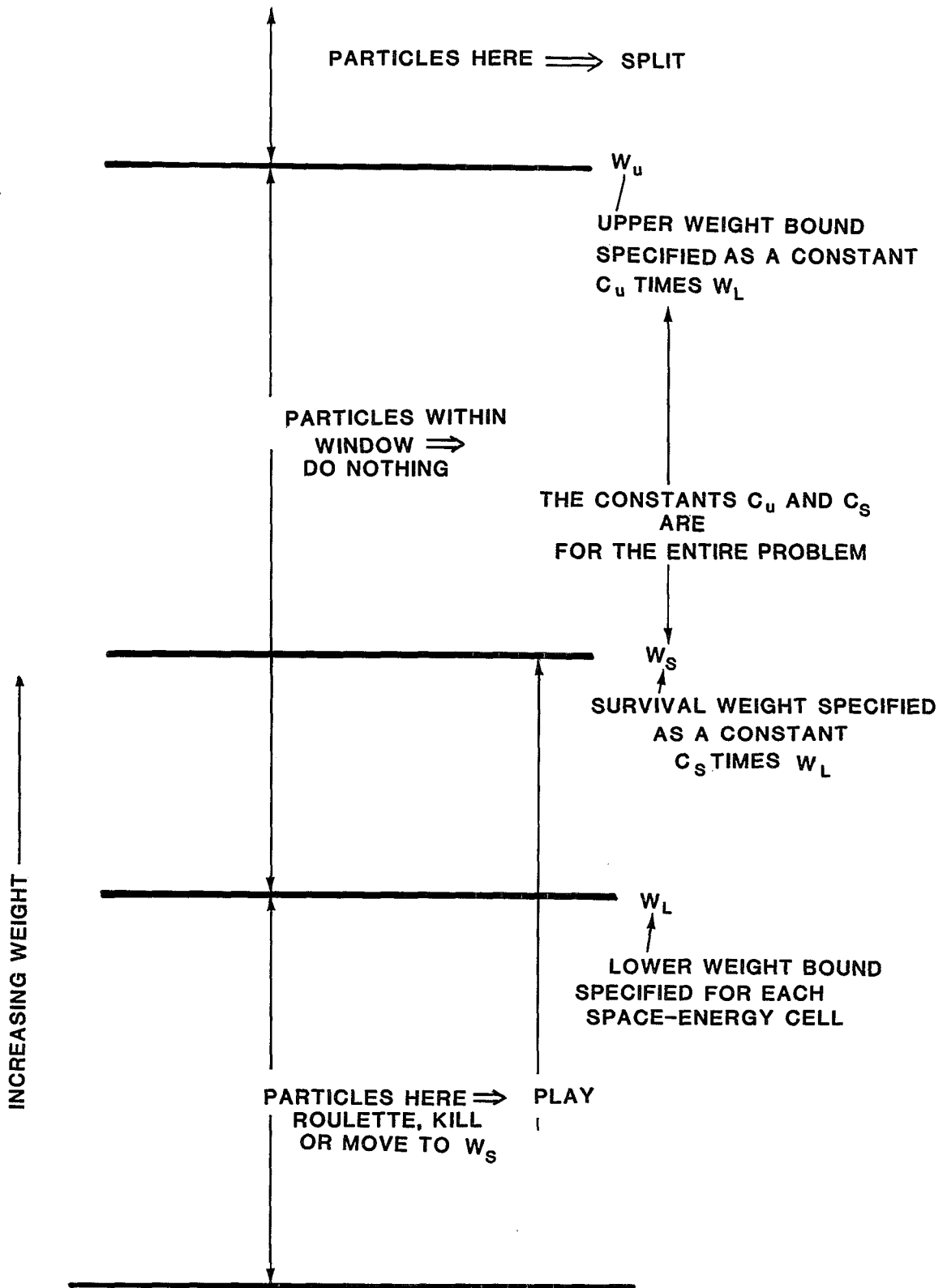


Fig. 30. Detail of the weight window.

LOWER BOUND = 0.5 / CELL IMPORTANCE WDWN 5 3 5

CELL PROGR PROBL	TRACKS ENTERING	POPULATION	COLLISIONS	COLLISIONS * WEIGHT (PER HISTORY)	NUMBER WEIGHTED ENERGY	FLUX WEIGHTED ENERGY	AVERAGE TRACK WEIGHT (RELATIVE)	AVERAGE TRACK MFP (CM)
2 2	52284	47147	122223	2.5784E+00	8.0176E-01	1.6607E+00	9.9061E-01	5.0620E+00
3 3	15527	10937	65628	1.2195E+00	4.1592E-01	1.0881E+00	8.8647E-01	4.1249E+00
4 4	9275	9759	55801	4.8096E-01	3.3695E-01	9.6786E-01	4.1114E-01	3.9027E+00
5 5	6744	9174	50117	1.6131E-01	3.1896E-01	1.0225E+00	1.5173E-01	3.9083E+00
6 6	5230	5994	32120	5.1613E-02	3.2700E-01	1.1480E+00	7.5598E-02	4.0113E+00
7 7	3561	4108	21736	1.7265E-02	3.4312E-01	1.2971E+00	3.7451E-02	4.1350E+00
8 8	2478	2807	14601	5.7387E-03	4.1889E-01	1.5625E+00	1.8594E-02	4.4885E+00
9 9	1833	2096	10746	2.1335E-03	4.7275E-01	1.7415E+00	9.3591E-03	4.6580E+00
10 10	1441	1596	8478	8.1523E-04	5.4895E-01	2.0562E+00	4.5771E-03	5.0049E+00
11 11	1362	1446	7522	3.4185E-04	5.6917E-01	2.0650E+00	2.1716E-03	5.1335E+00
12 12	1233	1258	6771	1.5712E-04	6.1261E-01	2.1111E+00	1.1042E-03	5.2412E+00
13 13	1183	1250	6324	6.8100E-05	6.2743E-01	2.0964E+00	5.2149E-04	5.2389E+00
14 14	1033	1347	6934	2.8037E-05	5.8460E-01	2.0346E+00	1.9258E-04	5.1695E+00
15 15	1095	1218	5960	1.1938E-05	6.4650E-01	2.1922E+00	9.5655E-05	5.3455E+00
16 16	1046	1161	5564	5.3848E-06	6.7465E-01	2.1922E+00	4.6191E-05	5.3729E+00
17 17	1005	1060	5159	2.4907E-06	6.9146E-01	2.2742E+00	2.3142E-05	5.4961E+00
18 18	1174	1204	6139	1.3226E-06	7.2900E-01	2.2244E+00	1.0671E-05	5.4990E+00
19 19	681	1330	5902	5.7313E-07	7.2447E-01	2.2032E+00	4.5460E-06	5.5027E+00
20 20	3186	10629	0	0.	1.2647E+00	3.3709E+00	4.8959E-07	1.0000+123
21 21	10006	20013	10379	5.6930E-12	1.6975E+00	4.0827E+00	5.6635E-10	7.4286E+02
22 22	946	946	0	0.	4.4692E-01	6.1713E-01	1.0980E-10	1.0000+123
TOTAL	122323	136480	448104	4.5183E+00				

NPS	TALLY 1			FOM	TALLY 4			FOM	TALLY 5			FOM
	MEAN	ERROR			MEAN	ERROR			MEAN	ERROR		
4000	7.03977E-08	.5470		7	1.60055E-14	.6033		6	8.83721E-18	.5702		7
8000	1.14310E-07	.6041		3	1.81517E-14	.5325		4	1.03267E-17	.5099		4
12000	7.62067E-08	.6041		2	1.21175E-14	.5319		2	6.89378E-18	.5092		3
16000	6.33715E-08	.5484		2	1.00078E-14	.4860		2	5.60263E-18	.4725		2
20000	6.31303E-08	.4782		2	1.06621E-14	.4331		2	5.70488E-18	.4198		2
24000	6.30845E-08	.4196		2	1.06500E-14	.3781		3	5.98017E-18	.3629		3
28000	6.22926E-08	.3761		2	1.01164E-14	.3480		3	5.75692E-18	.3320		3
32000	6.28397E-08	.3361		2	1.05989E-14	.3154		3	5.79892E-18	.3019		3
36000	6.30160E-08	.3143		2	1.06457E-14	.2958		3	5.88347E-18	.2840		3
40000	5.93140E-08	.3018		2	1.01066E-14	.2819		3	5.59554E-18	.2706		3
44000	5.59769E-08	.2928		2	9.92630E-15	.2661		3	5.43684E-18	.2589		3
46770	5.86550E-08	.2681		3	1.04766E-14	.2435		3	5.82362E-18	.2347		3

DUMP NO. 2 ON FILE RUNTPE NPS = 46770 CTM = 4.60

FOM 3 HERE AND 4 FOR SPLITTING DIRECTLY, BUT STATISTICS ARE BAD

Fig. 31. Window (space only) from importances.

4. ring detector, and
5. spatial weight window from refined cell importances.

Figure 31 shows the spatial weight window results. Comparison with Fig. 23 shows that the FOM (tally 1) is 3 for the weight window versus 4 for geometry splitting, but the statistics are bad on both runs. The main point is that a spatial weight window and geometry splitting give comparable results. In fact, in most cases where the statistics are good enough to judge, a spatial window is marginally superior to geometry splitting.

XIV. THE WEIGHT WINDOW GENERATOR

The weight window generator semiautomatically obtains optimized weight windows. The generator can be very useful for experienced Monte Carlo users; it is not recommended for novices. Weight window generator details are described in the September 16, 1982, X-6 memo, titled "Use of the Weight Window Generator."

A. Comments

1. The generator requires considerable user understanding and *intervention* to work effectively.
2. The generator is scheduled to become a standard MCNP feature, but is currently only a standard (maintained) patch to MCNP.
3. Running MCNP with the generator typically costs an extra 20-50% of the required time for running MCNP without the generator.
4. Tracking is not affected by the generator; that is, every particle executes a random walk identical to its random walk when the generator is not used.

B. Importance Generator Theory

The importance of a particle at a point P in phase-space is equal to the expected score a unit weight particle will generate. Imagine dividing the phase-space into a number of phase-space "cells" or regions. The importance of a cell can then be defined as the expected score generated by a unit weight particle after entering the cell. Thus with a little bookkeeping, the cell's importance can be estimated as

$$\text{Importance (expected score)} = \frac{\text{total score because of particles (and their progeny) entering the cell}}{\text{total weight entering the cell}}$$

Consider the example of Fig. 32, which represents a generic phase-space geometry of four cells. In this example, the capture probability at each collision is 0.5, and capture is treated implicitly by weight reduction in conjunction with a weight cutoff. Particles are born in cell 1 and are scored as they leave the slab from cell 4. The S values are used to determine the splitting and Russian roulette games played at boundary crossings between the four phase-space cells. In practice, these S values are usually the user's best initial guess at an importance function. Each particle trajectory is consecutively numbered. Table III shows the importance estimation process for the three particle histories of Fig. 32. Note also that this importance estimation works regardless of the variance reduction techniques used during the calculation (tracks that reenter the same phase-space cell should not be counted twice as weight entering).

C. Setting the Weight Window from the Estimated Importances

Although the generator and weight window concepts are independent, they are complementary. One cannot

TABLE III. Importance Estimation Process for Particle Histories in Fig. 32.

Row	Description	Cell 1	Cell 2	Cell 3	Cell 4
Weight					
1	Trajectories entering	1, 8, 13	3, 4, 9, 10	14, 15	6, 17
2	Weight entering associated with above trajectories	1, 1, 1	0.25, 0.25, 0.5, 0.5	0.5, 0.5	0.5, 0.5
3	Total weight entering	3	1.5	1	1
Score					
4	Trajectories entering that resulted in score	7, 17	7	17	7, 17
5	Scores associated with above trajectories	0.25, 0.5	0.25	0.5	0.25, 0.5
6	Total score	0.75	0.25	0.5	0.75
Estimate					
7	Estimated importance Row 6/Row 3	0.25	0.167	0.5	0.75

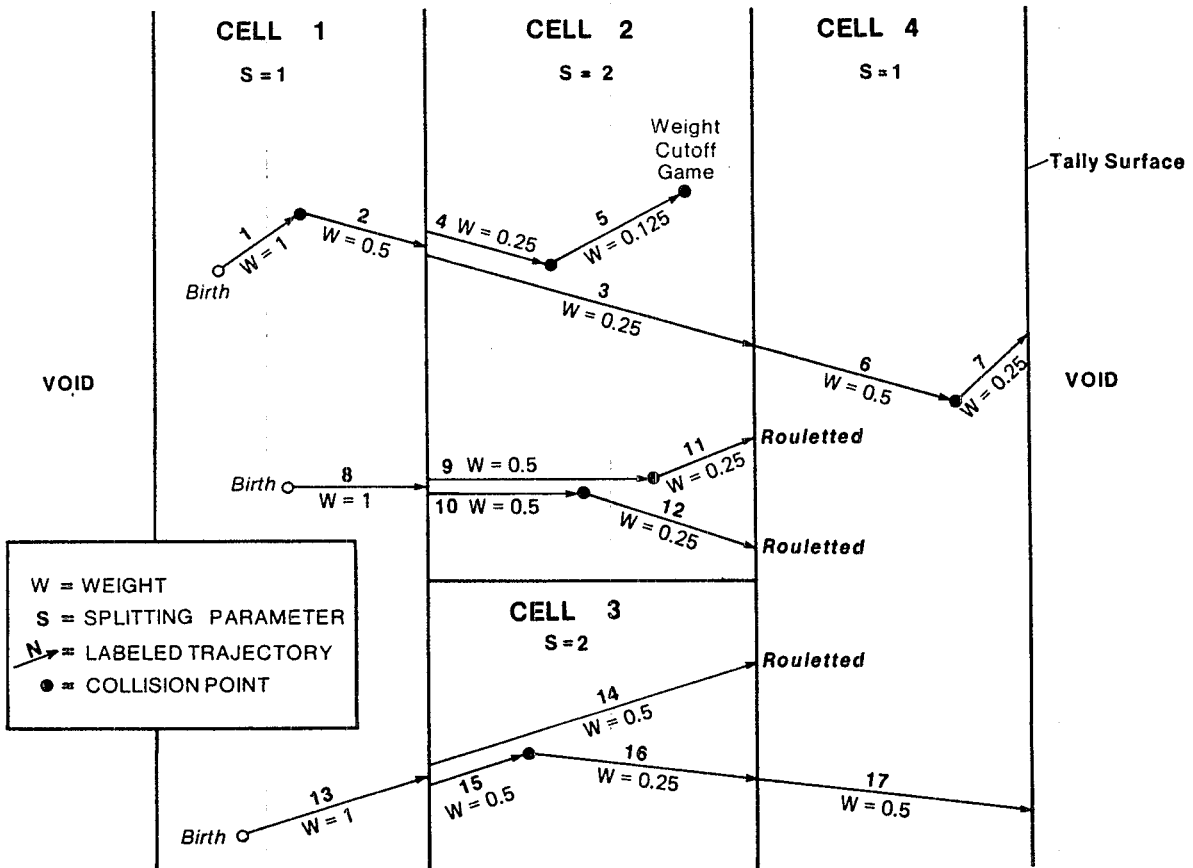


Fig. 32. Generic Monte Carlo problem of four cells with three particle histories, illustrating how importances can be estimated.

insist that every history contribute the same score (a zero variance solution), but by using a window inversely proportional to the importance, one can insist that the mean score from any track in the problem be roughly constant. In other words, the window is chosen so that the track weight times the mean score (for unit track weight) is approximately constant. Under these conditions, the variance is caused mostly by the variation in the number of contributing tracks rather than by the variation in track score.

Thus far, two weight window properties remain unspecified, the constant of inverse proportionality and the width of the window. Empirically, it has been observed that an upper weight bound five times the lower weight bound works well, but the results are reasonably insensitive to this choice anyway. The constant of inverse proportionality is chosen so that the lower weight bound in some reference cell is chosen appropriately. For example, in the problem described here, the constant was chosen so that the lower weight bound in the source cell was 0.5. The source particles were of unit

weight, so they all started within the (0.5-2.5) window. In most instances the constant should be chosen this way so the source particles start within the window.

D. Spatial Generator Results

Figure 33 is the same run as Fig. 31 except that the generator is turned on. Note that the runs track perfectly and the generator has slowed the calculation by 4%. Typically, the generator will slow the calculation by 20-50%, but of course the generator can be turned off when a good weight window has been generated. Thus no time penalty need be paid for the final run to grind the statistics down.

Figure 34 shows the generated spatial weight window inserted in the input file for the next run. Many windows will be displayed, so I will explain how to interpret the WFN card entries, lines 67-72. Line 67 indicates that the first (and here the only) neutron weight window has an upper energy range of 100 MeV. If there were more

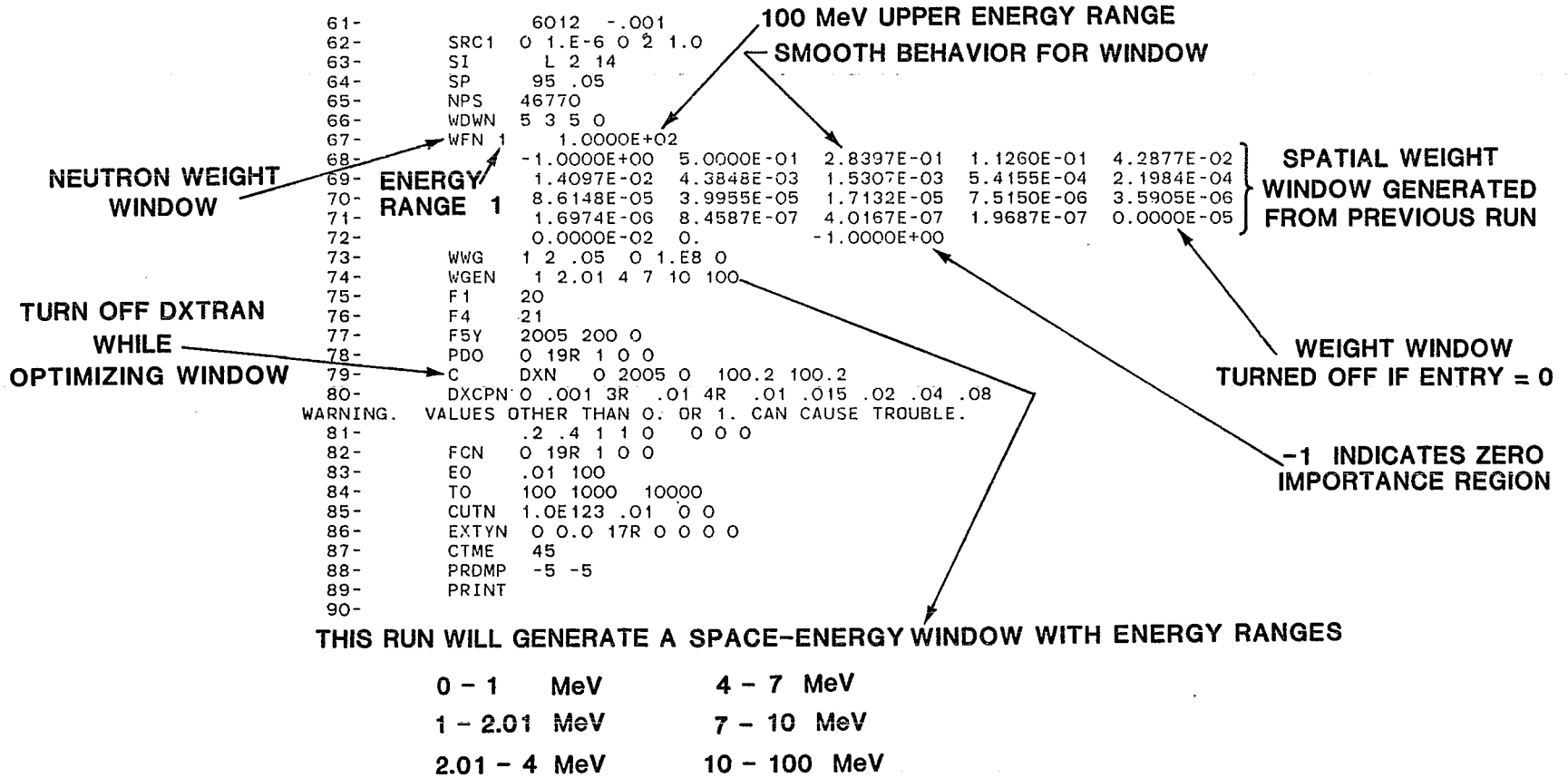


Fig. 34. Input for generating space-energy window.

energy ranges, the upper energy bound for the i^{th} window would be the lower energy bound for the $i + 1^{\text{st}}$ window. The lower energy bound for the first window is always zero. Lines 68 to 72 are the lower weight bounds for cells 1 to 23 and read, in order, from left to right and top to bottom. For example, the lower weight bound in cell 15 is 3.5905E-06. A zero lower weight bound turns off the weight window and a -1 indicates a zero importance region where the particle is terminated upon entering.

Earlier, I cautioned that user intervention is required. This intervention can be seen in the WFN1 entries (Fig. 34) for cells 20-22 where I turned off the weight window game by entering zeros because I did not want to use the window in this highly angle-dependent part of the problem. The window behaved smoothly, falling off roughly by factors of 2; thus the weight window needed no further intervention.

E. Generating a Space-Energy Weight Window

As mentioned earlier, the spatial weight window of Fig. 34 looks reasonable and is probably about as good as it will get. Furthermore, experience has proved biasing in the energy domain to be quite important. Therefore, the generator was employed, using the input shown in Fig. 34, to generate a space-energy window. The energy ranges chosen were

0	—	1	MeV
1	—	2.01	MeV
2.01	—	4	MeV
4	—	7	MeV
7	—	10	MeV
10	—	100	MeV

The choices were based mostly on experience and not on detailed analysis nor on inspiration. In particular, note that factors of 2 pervade the Monte Carlo choices. Note (line 79) that DXTRAN has been turned off while a space-energy window is generated (C indicates a comment card). This is perfectly reasonable because the space-energy window will be used to penetrate the concrete and will therefore be optimized for tally 1; DXTRAN is used to improve tallies 4 and 5 but not tally 1.

Figure 35 summarizes the run that used the spatial window of Fig. 34 to produce a space-energy window (Fig. 36). Note that removing DXTRAN allowed many more particles to be run.

F. Discussion of the Generated Space-Energy Window

The space-energy window produced is shown in Fig. 36. Wherever a zero entry appears, it means that the

generator was unable to estimate importance for that space-energy cell because no particle ever left these space-energy cells and contributed to tally 1. Note that the zero entries are usually far from the tally surface and low in energy, indicating that low-energy particles far from the tally surface have a hard time tallying, as expected. If a zero is left as an entry, then no weight window game will be played, an undesirable situation; thus the user must supply nonzero weight windows.

Figure 37 shows how I adjusted the weight windows. An adjusted window entry is indicated by three trailing zeros in the entry. The window was adjusted according to two general patterns observed from Fig. 36. If W_{ij} is the lower weight bound in energy region i and spatial cell j , then these two general patterns can be expressed as $W_{ij} < W_{i-m,j}$ and $W_{ij} < W_{i,j-n}$, where m and n are positive integers. Thus Fig. 37 was obtained by interpolation and extrapolation from Fig. 36.

G. Results Using the Space-Energy Weight Window

The space-energy window of Fig. 37 was inserted in the input file; Fig. 38 shows the results. Tally 1 has improved nicely from an FOM of 6 to 43. However, note in the middle of Fig. 38 that the source particles are not starting within the window, indicating that the source should be biased so that the source particles start in the weight window.

The window (in source cell 2) for 2-MeV particles is 9 to 45, (recall that the upper bound is 5 times the lower bound) (Fig. 37), whereas the window for 14-MeV particles is .05 to .25. Recall (Fig. 36) that previous source energy biasing gave source weights of 9.5 and 0.055 at 2 MeV and 14 MeV, respectively. From this lucky coincidence we already know the proper source biasing. Without this coincidence, one could experiment with different source energy biasing until the last column of Fig. 36 indicated source weights within the window.

H. Results Using Space-Energy Window and Source Energy Bias

Figure 39 shows the effect of starting the source particles within the window; the FOM for tally 1 improves from 43 (Fig. 38) to 75. The only peculiar thing in Fig. 39 is the sudden rise and fall in the "tracks entering" and "population" columns around cells 6 and 7. A re-examination (see Fig. 37) of the adjusted space-energy window reveals that the window for cell 6 in the sixth energy range looks wrong; it does not fit the general pattern. This entry was altered from 3.4489E-04 to 2.2000E-3. Also, the window for cell 16 in the second energy range was altered from 4.5208E-6 to 1.0000E-5. Although cell 16's window was not responsible for the

THIS RUN GENERATED A SPACE-ENERGY WEIGHT WINDOW

CELL PROGR PROBL	TRACKS ENTERING	POPULATION	COLLISIONS	COLLISIONS * WEIGHT (PER HISTORY)	NUMBER WEIGHTED ENERGY	FLUX WEIGHTED ENERGY	AVERAGE TRACK WEIGHT (RELATIVE)	AVERAGE TRACK MFP (CM)
2 2	31563	28369	73109	2.5609E+00	8.0044E-01	1.6463E+00	9.9001E-01	5.0488E+00
3 3	9235	6559	39580	1.2364E+00	4.0437E-01	1.0730E+00	8.9203E-01	4.0870E+00
4 4	5318	5726	31791	4.5867E-01	3.3009E-01	9.7941E-01	4.1401E-01	3.8937E+00
5 5	4689	5964	32365	1.5856E-01	3.1409E-01	1.0067E+00	1.3957E-01	3.8815E+00
6 6	4428	5792	31037	5.1074E-02	3.1464E-01	1.1052E+00	4.6976E-02	3.9459E+00
7 7	4198	5609	29062	1.5737E-02	3.3910E-01	1.2547E+00	1.5437E-02	4.1301E+00
8 8	4292	5635	28558	5.0913E-03	3.8529E-01	1.4915E+00	5.0716E-03	4.3485E+00
9 9	4005	5375	27348	1.7710E-03	4.5086E-01	1.7681E+00	1.8445E-03	4.6537E+00
10 10	4335	4679	23179	6.5910E-04	5.3091E-01	1.9515E+00	8.2099E-04	4.9305E+00
11 11	4010	5243	26509	2.8124E-04	5.4582E-01	1.9532E+00	3.0345E-04	4.9764E+00
12 12	4571	4918	24772	1.1931E-04	5.7551E-01	2.0257E+00	1.3936E-04	5.1013E+00
13 13	4215	5480	27612	4.8943E-05	5.9478E-01	2.0723E+00	5.0869E-05	5.1656E+00
14 14	4451	4942	24393	2.1525E-05	6.0769E-01	2.0889E+00	2.5386E-05	5.2023E+00
15 15	3971	4415	22316	9.8004E-06	5.9963E-01	2.0263E+00	1.2641E-05	5.1988E+00
16 16	3251	4140	20789	4.3415E-06	6.1546E-01	2.0906E+00	6.0496E-06	5.2793E+00
17 17	3582	3808	19422	2.0380E-06	6.2432E-01	2.0520E+00	3.0269E-06	5.2785E+00
18 18	3023	3244	16161	8.7591E-07	6.5356E-01	2.0774E+00	1.5639E-06	5.3515E+00
19 19	1772	2568	10985	3.4732E-07	6.7128E-01	2.1300E+00	8.9100E-07	5.4105E+00
20 20	1155	1154	0	0.	1.4029E+00	3.3493E+00	8.9086E-07	1.0000+123
21 21	5	10	5	1.8217E-12	6.5340E+00	8.3827E+00	3.7267E-07	8.6976E+02
22 22	0	0	0	0.	0.	0.	0.	0.
TOTAL	106669	113630	508993	4.4893E+00				

NPS	TALLY 1			FOM	TALLY 4			FOM	TALLY 5			FOM
	MEAN	ERROR			MEAN	ERROR			MEAN	ERROR		
2000	4.42065E-08	.7235		5	0.	0.0000		0	0.	0.0000		0
4000	3.48294E-08	.5557		4	0.	0.0000		0	0.	0.0000		0
6000	2.63453E-08	.5039		4	0.	0.0000		0	0.	0.0000		0
8000	2.71267E-08	.4092		4	0.	0.0000		0	0.	0.0000		0
10000	2.20586E-08	.4029		4	0.	0.0000		0	0.	0.0000		0
12000	2.65686E-08	.3186		5	0.	0.0000		0	0.	0.0000		0
14000	3.06192E-08	.2893		5	0.	0.0000		0	0.	0.0000		0
16000	2.77965E-08	.2812		5	1.78371E-15	1.0000		0	0.	0.0000		0
18000	3.04967E-08	.2519		5	1.58552E-15	1.0000		0	0.	0.0000		0
20000	3.35645E-08	.2332		5	5.72437E-15	.7910		0	1.89637E-18	1.0000		0
22000	3.12439E-08	.2286		5	5.20397E-15	.7910		0	1.72397E-18	1.0000		0
24000	3.07538E-08	.2168		5	4.77030E-15	.7910		0	1.58031E-18	1.0000		0
26000	3.13077E-08	.2077		5	4.40336E-15	.7910		0	1.45875E-18	1.0000		0
28000	3.61601E-08	.1885		6	5.10598E-15	.6640		0	1.96601E-18	.7559		0
28144	3.65780E-08	.1861		6	5.07986E-15	.6640		0	1.95595E-18	.7559		0

MEAN LOW AND
NO DXTRAN WORK

NOTE INCREASE FROM 2
WITH IMPORTANCES USED.

TIME = 4.63 MINUTES

Fig. 35. Spatial window with no DXTRAN.

WFN 1	1.0000E+00				
	-1.0000E+00	0.	0.	0.	0.
	0.	0.	0.	0.	0.
	0.	0.	0.	0.	1.4100E-04
	8.1682E-05	7.4357E-06	1.6792E-06	6.8234E-07	0.
	0.	0.	-1.0000E+00		
WFN 2	2.0100E+00				
	-1.0000E+00	0.	0.	0.	0.
	0.	0.	0.	0.	0.
	1.2125E-02	5.0272E-03	7.6270E-04	1.0793E-04	3.9958E-05
	4.5208E-06	2.5657E-06	7.6579E-07	2.7840E-07	0.
	0.	0.	-1.0000E+00		
WFN 3	4.0000E+00				
	-1.0000E+00	0.	1.1223E-01	4.8144E-02	2.4881E-02
	8.1246E-03	4.7221E-03	2.0442E-03	7.1146E-04	3.9582E-04
	1.5468E-04	6.2149E-05	2.1354E-05	9.6969E-06	4.0856E-06
	1.8644E-06	8.4843E-07	3.9794E-07	2.0447E-07	0.
	0.	0.	-1.0000E+00		
WFN 4	7.0000E+00				
	-1.0000E+00	0.	1.6534E-02	1.1285E-02	5.3483E-03
	2.9056E-03	9.7180E-04	2.1018E-04	2.5524E-04	1.3185E-04
	5.1451E-05	9.6495E-06	1.1916E-05	3.8168E-06	2.4425E-06
	1.1805E-06	6.2537E-07	3.7240E-07	1.9655E-07	0.
	0.	0.	-1.0000E+00		
WFN 5	1.0000E+01				
	-1.0000E+00	0.	1.1635E-02	4.1318E-03	3.4173E-03
	2.3599E-03	1.0721E-03	1.5395E-04	1.4119E-04	7.6465E-05
	3.8697E-05	2.1199E-05	1.0413E-05	5.3956E-07	2.6293E-06
	1.5106E-06	2.6978E-07	1.3489E-07	1.8884E-07	0.
	0.	0.	-1.0000E+00		
WFN 6	1.0000E+02				
	-1.0000E+00	5.0000E-02	1.3488E-02	1.0148E-02	4.7609E-03
	3.4489E-04	1.1949E-03	6.2029E-05	2.1723E-04	8.2253E-05
	5.7428E-05	2.8461E-06	1.0432E-05	4.6621E-06	2.2761E-06
	1.2537E-06	7.1526E-07	2.6978E-07	2.1982E-07	0.
	0.	0.	-1.0000E+00		

Fig. 36. Space-energy weight window produced.

WFN 1	1.0000E+00				
	-1.0000E+00	2.6000E+01	2.6000E+01	8.6000E+00	2.9000E+00
	9.6000E-01	3.2000E-01	1.1000E-01	3.5000E-02	1.2000E-02
	3.9000E-03	1.3000E-03	4.4000E-04	1.5000E-04	4.9000E-05
	1.6000E-05	5.4000E-06	1.8000E-06	6.0000E-07	0.
	0.	0.	-1.0000E+00		
WFN 2	2.0100E+00				
	-1.0000E+00	9.0000E+00	4.5000E+00	2.3000E+00	1.1000E+00
	5.6000E-01	2.8000E-01	1.4000E-01	7.0000E-02	3.5000E-02
	1.2125E-02	5.0272E-03	7.6270E-04	1.6000E-04	3.9958E-05
	4.5208E-06	2.5657E-06	7.6579E-07	2.7840E-07	0.
	0.	0.	-1.0000E+00		
WFN 3	4.0000E+00				
	-1.0000E+00	3.0000E-01	1.1223E-01	4.8144E-02	2.4881E-02
	8.1246E-03	4.7221E-03	2.0442E-03	7.1146E-04	3.9582E-04
	1.5468E-04	6.2149E-05	2.1354E-05	9.6969E-06	4.0856E-06
	1.8644E-06	8.4843E-07	3.9794E-07	2.0447E-07	0.
	0.	0.	-1.0000E+00		
WFN 4	7.0000E+00				
	-1.0000E+00	5.0000E-02	1.6534E-02	1.1285E-02	5.3483E-03
	2.9056E-03	9.7180E-04	5.0000E-04	2.5524E-04	1.3185E-04
	5.1451E-05	2.5000E-05	1.1916E-05	5.0000E-06	2.4425E-06
	1.1805E-06	6.2537E-07	3.7240E-07	1.9655E-07	0.
	0.	0.	-1.0000E+00		
WFN 5	1.0000E+01				
	-1.0000E+00	5.0000E-02	1.1635E-02	4.1318E-03	3.4173E-03
	2.3599E-03	1.0721E-03	4.0000E-04	1.4119E-04	7.6465E-05
	3.8697E-05	2.1199E-05	1.0413E-05	5.0000E-06	2.6293E-06
	1.5106E-06	5.0000E-07	2.0000E-07	1.0000E-07	0.
	0.	0.	-1.0000E+00		
WFN 6	1.0000E+02				
	-1.0000E+00	5.0000E-02	1.3488E-02	1.0148E-02	4.7609E-03
	3.4489E-04	1.1949E-03	5.0000E-04	2.1723E-04	8.2253E-05
	5.7428E-05	2.0000E-05	1.0432E-05	4.6621E-06	2.2761E-06
	1.2537E-06	7.1526E-07	2.6978E-07	1.0000E-07	0.
	0.	0.	-1.0000E+00		

Fig. 37. Adjusted (by hand) space-energy weight window. Look for three zeros as indication of hand adjustment.

LEDGER OF NET NEUTRON CREATION AND LOSS (FOR ACCOUNTING ONLY)

	TRACKS	WEIGHT (PER SOURCE PARTICLE)	ENERGY (PER SOURCE PARTICLE)		TRACKS	WEIGHT (PER SOURCE PARTICLE)	ENERGY (PER SOURCE PARTICLE)
SOURCE	79266	1.0000E+00	2.6006E+00	ESCAPE	50305	7.6849E-01	1.6402E+00
SCATTERING	0	0.	0.	SCATTERING	0	0.	8.7143E-01
FISSION	0	0.	0.	CAPTURE	18796	9.1107E-03	9.5665E-02
(N,XN)	428	3.4146E-04	7.8500E-04	ENERGY CUTOFF	6783	2.2893E-01	1.2512E-03
FORCED COLLISION	30	0.	0.	TIME CUTOFF	0	0.	0.
WEIGHT CUTOFF	0	0.	0.	WEIGHT CUTOFF	0	0.	0.
WEIGHT WINDOW	95295	9.4426E-01	1.1818E+00	WEIGHT WINDOW	99135	9.3807E-01	1.1746E+00
CELL IMPORTANCE	0	0.	0.	CELL IMPORTANCE	0	0.	0.
ENERGY IMPORT.	0	0.	0.	ENERGY IMPORT.	0	0.	0.
DXTRAN	0	0.	0.	DXTRAN	0	0.	0.
EXP. TRANSFORM	0	0.	0.	EXP. TRANSFORM	0	0.	0.
TOTAL	175019	1.9446E+00	3.7831E+00	DEAD FISSIION	0	0.	0.
				TOTAL	175019	1.9446E+00	3.7831E+00

PREDICTED AVG OF SRC FUNCTION ZERO 2.6000E+00
 TRACKS PER NEUTRON STARTED 2.2080E+00
 COLLISIONS PER NEUTRON STARTED 5.4481E+00
 TOTAL COLLISIONS 431852
 NET MULTIPLICATION 1.0003E+00 .0001

AVERAGE LIFETIME, SHAKES
 ESCAPE 5.1106E-01
 CAPTURE 9.3320E-01
 CAPTURE OR ESCAPE 5.1601E-01
 ANY TERMINATION 1.5297E+00

CUTOFFS
 TCD 1.0000+123
 ECD 1.0000E-02
 WC1 0.
 WC2 0.

COMPUTER TIME SO FAR IN THIS RUN 4.67 MINUTES
 COMPUTER TIME IN MCRUN (4C0) 4.61 MINUTES
 SOURCE PARTICLES PER MINUTE 1.7198E+04
 FIELD LENGTH 376688 = 1337560B
 RANDOM NUMBERS GENERATED 4305494
 LAST STARTING RANDOM NUMBER 0527527715031145B
 NEXT STARTING RANDOM NUMBER 6032700471631661B

TOTAL NEUTRONS BANKED 72558
 PER SOURCE PARTICLE 9.1537E-01
 TOTAL PHOTONS BANKED 0
 PER SOURCE PARTICLE 0.
 MAXIMUM NUMBER EVER IN BANK 16
 BANK OVERFLOWS TO DISK 0

3967 SOURCE PARTICLES HAD WEIGHT ABOVE WINDOW.
 BY INCREASING WW ENERGY INTERVAL: 0 0 0 0 0 3967

WINDOW DOING WHAT SOURCE
 BIASING OUGHT TO BE DOING

75299 SOURCE PARTICLES HAD WEIGHT BELOW WINDOW.
 BY INCREASING WW ENERGY INTERVAL: 0 75299 0 0 0 0

NOTE IMPROVEMENT FROM FOM = 6 AND LOW MEAN

NPS	TALLY 1			FOM	TALLY 4			FOM	TALLY 5			FOM
	MEAN	ERROR	FOM		MEAN	ERROR	FOM		MEAN	ERROR	FOM	
4000	4.26255E-08	.3126	40	0.	0.0000	0	0.	0.0000	0			
8000	3.93201E-08	.2170	44	1.80090E-15	.9999	2	1.25350E-18	.9999	2			
12000	3.62294E-08	.1831	45	3.75877E-15	.7518	2	8.35669E-19	1.0000	1			
16000	3.78523E-08	.1531	48	2.81908E-15	.7518	2	6.26752E-19	1.0000	1			
20000	3.84399E-08	.1436	43	2.25526E-15	.7518	1	5.01402E-19	1.0000	0			
24000	3.69001E-08	.1348	42	1.87939E-15	.7518	1	4.17835E-19	1.0000	0			
28000	3.74802E-08	.1250	42	1.61090E-15	.7518	1	3.58144E-19	1.0000	0			
32000	3.96024E-08	.1155	42	2.62570E-15	.5210	2	1.65752E-18	.6340	1			
36000	3.95712E-08	.1078	43	3.35794E-15	.4230	2	1.73638E-18	.5536	1			
40000	3.96848E-08	.1022	43	3.02214E-15	.4230	2	1.56274E-18	.5536	1			
44000	4.01664E-08	.0973	43	3.62170E-15	.4015	2	1.80785E-18	.4849	1			
48000	4.08935E-08	.0922	43	3.31989E-15	.4015	2	1.65720E-18	.4849	1			
52000	4.31095E-08	.0878	43	3.66148E-15	.3735	2	1.93062E-18	.4367	1			
56000	4.41742E-08	.0837	43	4.82611E-15	.3394	2	2.66350E-18	.3921	1			
60000	4.45244E-08	.0808	43	4.50437E-15	.3394	2	2.48593E-18	.3921	1			
64000	4.44663E-08	.0790	43	5.16357E-15	.3074	2	2.84505E-18	.3458	2			
68000	4.42586E-08	.0764	43	6.64840E-15	.2779	3	3.37077E-18	.3108	2			
72000	4.50210E-08	.0742	43	8.14304E-15	.2465	3	4.31000E-18	.2738	3			
76000	4.46087E-08	.0720	43	8.58957E-15	.2296	4	4.42186E-18	.2586	3			
79266	4.48032E-08	.0704	43	8.23565E-15	.2296	4	4.23966E-18	.2586	3			

TIME = 4.61 MIN

Fig. 38. Space-energy window.

BIASED SOURCE
 10% AT 2 MeV
 90% AT 14 MeV

CELL	TRACKS ENTERING	POPULATION	COLLISIONS	COLLISIONS * WEIGHT (PER HISTORY)	NUMBER WEIGHTED ENERGY	FLUX WEIGHTED ENERGY	AVERAGE TRACK WEIGHT (RELATIVE)	AVERAGE TRACK MFP (CM)		
PROGR	PROBL	WHAT HAPPENED								
2	2	72900	?	71569	64844	2.5985E+00	7.9765E-01	1.6550E+00	1.4970E+00	5.0683E+00
3	3	13967		13065	22767	1.3658E+00	3.8362E-01	1.0424E+00	1.8665E+00	4.0300E+00
4	4	6869		11224	18913	4.4432E-01	3.2624E-01	1.0203E+00	6.7267E-01	3.9124E+00
5	5	6189		10196	16387	1.6382E-01	2.9485E-01	9.9241E-01	2.8660E-01	3.8271E+00
6	6	5776		20034	26603	5.2169E-02	3.0415E-01	1.1445E+00	5.2098E-02	3.9416E+00
7	7	10695		11731	18387	1.3503E-02	3.2685E-01	1.4222E+00	2.2751E-02	4.1834E+00
8	8	6713		9403	15363	5.0785E-03	3.4114E-01	1.6170E+00	1.0314E-02	4.3812E+00
9	9	5685		9455	15729	1.6771E-03	5.5594E-01	2.0278E+00	3.7507E-03	4.8771E+00
10	10	5692		9068	15237	7.4597E-04	5.8661E-01	2.1211E+00	1.6788E-03	4.9174E+00
11	11	5420		9177	16089	2.3916E-04	7.5402E-01	2.5748E+00	5.7359E-04	5.4790E+00
12	12	5645		8902	16326	1.1446E-04	7.1401E-01	2.5327E+00	2.6741E-04	5.4651E+00
13	13	5922		9225	18071	5.4526E-05	7.8201E-01	2.4512E+00	1.1940E-04	5.4770E+00
14	14	6118		8851	18914	2.7250E-05	6.7606E-01	2.2546E+00	5.9161E-05	5.2972E+00
15	15	5950		9320	20500	1.1794E-05	6.4999E-01	2.2862E+00	2.4826E-05	5.3760E+00
16	16	6488		9782	25896	5.2562E-06	6.6610E-01	2.3080E+00	9.7062E-06	5.4234E+00
17	17	7228		10092	28621	2.5251E-06	6.5633E-01	2.2104E+00	4.4270E-06	5.3554E+00
18	18	7192		10409	31844	1.1580E-06	6.3917E-01	2.1387E+00	1.9383E-06	5.3137E+00
19	19	5451		9074	29875	4.5332E-07	7.1276E-01	2.2535E+00	8.8928E-07	5.4711E+00
20	20	4670		4665	0	0.	1.2199E+00	3.3018E+00	7.5707E-07	1.0000+123
21	21	21		42	22	6.7924E-12	1.2606E+00	3.1874E+00	2.7759E-07	6.0228E+02
22	22	4		4	0	0.	6.7857E-02	2.1071E-01	4.5584E-08	1.0000+123
TOTAL		194595		255288	420388	4.6460E+00				

NATURAL SOURCE
 95% AT 2 MeV
 5% AT 14 MeV

NPS	TALLY 1			FOM	TALLY 4			FOM	TALLY 5			FOM
	MEAN	ERROR			MEAN	ERROR			MEAN	ERROR		
4000	5.57495E-08	.2280	68	6.34674E-15	.7133	6	4.22938E-18	.7305	6			
8000	4.56612E-08	.1668	69	2.30878E-14	.6567	4	3.30529E-17	.6802	4			
12000	4.36483E-08	.1478	61	1.72329E-14	.5962	3	2.34337E-17	.6424	3			
16000	4.67028E-08	.1221	66	1.44250E-14	.5443	3	1.75753E-17	.6424	2			
20000	4.79930E-08	.1048	71	1.37601E-14	.4705	3	1.48115E-17	.6120	2			
24000	5.24382E-08	.0916	76	1.48934E-14	.4291	3	2.37583E-17	.5761	1			
28000	5.18837E-08	.0848	77	1.27658E-14	.4291	3	2.03643E-17	.5761	1			
32000	4.95469E-08	.0794	77	1.16204E-14	.4143	2	1.79888E-17	.5708	1			
36000	5.12823E-08	.0741	76	1.12201E-14	.3896	2	1.63018E-17	.5602	1			
40000	5.27996E-08	.0691	78	1.06390E-14	.3733	2	1.46716E-17	.5602	1			
44000	5.06052E-08	.0667	77	1.01628E-14	.3585	2	1.33378E-17	.5602	1			
48000	4.92408E-08	.0640	78	9.92531E-15	.3420	2	1.27618E-17	.5383	1			
52000	4.87547E-08	.0623	76	9.43925E-15	.3333	2	1.18694E-17	.5343	1			
56000	5.06014E-08	.0599	76	8.76501E-15	.3333	2	1.10216E-17	.5343	0			
60000	4.98803E-08	.0581	76	8.18068E-15	.3333	2	1.02868E-17	.5343	0			
64000	4.98051E-08	.0565	75	8.55026E-15	.3084	2	1.01502E-17	.5090	0			
68000	4.94767E-08	.0548	75	8.04731E-15	.3084	2	9.55314E-18	.5090	0			
71167	4.91626E-08	.0536	75	8.47612E-15	.2875	2	9.19833E-18	.5052	0			

NOTE IMPROVEMENT

TIME = 4.61 MIN

Fig. 39. Space-energy window and source energy bias.

peculiarity, 10^{-5} just looked more reasonable because in energy range 2, the windows were decreasing by factors of 4. Figure 40 shows the corrected window.

Figure 41 shows the results of correcting the bad window. The "tracks entering" and "population" columns look much better. Perversely, the FOM decreases, but the decrease is not statistically significant and the corrected window was used for subsequent runs.

I. Exponential Source Angle Biasing and the Weight Window

Recall that exponential source angle biasing did not improve the FOMs for the problem. As with most biasing techniques, competing factors affect calculation. Exponential source angle biasing preferentially samples source neutrons moving close to the $+\hat{y}$ direction. Thus source neutrons that are more likely to score are sampled more often. However, the biasing also introduces a weight fluctuation that the geometry splitting/Russian roulette technique preserves. Probably the negative ef-

fects of this weight fluctuation cancelled the benefit of sampling more important source neutrons more often.

A conference participant (John Hendricks, Los Alamos) suggested that the exponential source angle biasing might have worked if it had been tried with the weight window technique rather than with geometry splitting/Russian roulette. He said that the weight window would probably alleviate the weight fluctuation problem; thus the exponential source angle biasing, in conjunction with the weight window, probably would improve the FOMs.

I agree with his assessment and include it here, without proof, as a good example of analyzing the interaction of different variance reduction techniques. However, the source angle biasing should not be expected to yield the same dramatic improvement in FOM as the source energy bias because the particles that tally will typically have many collisions and will quickly forget their source angle. In other words, after a few collisions, a preferred source particle will be essentially identical (except possibly its weight) to an unpreferred

	WFN 1	1.0000E+00							
		-1.0000E+00	2.6000E+01	2.6000E+01	8.6000E+00	2.9000E+00			
		9.6000E-01	3.2000E-01	1.1000E-01	3.5000E-02	1.2000E-02			
		3.9000E-03	1.3000E-03	4.4000E-04	1.5000E-04	4.9000E-05			
		1.6000E-05	5.4000E-06	1.8000E-06	6.0000E-07	0.			
		0.	0.	-1.0000E+00					
	WFN 2	2.0100E+00							
		-1.0000E+00	9.0000E+00	4.5000E+00	2.3000E+00	1.1000E+00			
		5.6000E-01	2.8000E-01	1.4000E-01	7.0000E-02	3.5000E-02			
		1.2125E-02	5.0272E-03	7.6270E-04	1.6000E-04	3.9958E-05			
ALTERED FROM 4.5208E-06		1.0000E-05	2.5657E-06	7.6579E-07	2.7840E-07	0.			
		0.	0.	-1.0000E+00					
	WFN 3	4.0000E+00							
		-1.0000E+00	3.0000E-01	1.1223E-01	4.8144E-02	2.4881E-02			
		8.1246E-03	4.7221E-03	2.0442E-03	7.1146E-04	3.9582E-04			
		1.5468E-04	6.2149E-05	2.1354E-05	9.6969E-06	4.0856E-06			
		1.8644E-06	8.4843E-07	3.9794E-07	2.0447E-07	0.			
		0.	0.	-1.0000E+00					
	WFN 4	7.0000E+00							
		-1.0000E+00	5.0000E-02	1.6534E-02	1.1285E-02	5.3483E-03			
		2.9056E-03	9.7180E-04	5.0000E-04	2.5524E-04	1.3185E-04			
		5.1451E-05	2.5000E-05	1.1916E-05	5.0000E-06	2.4425E-06			
		1.1805E-06	6.2537E-07	3.7240E-07	1.9655E-07	0.			
		0.	0.	-1.0000E+00					
	WFN 5	1.0000E+01							
		-1.0000E+00	5.0000E-02	1.1635E-02	4.1318E-03	3.4173E-03			
		2.3599E-03	1.0721E-03	4.0000E-04	1.4119E-04	7.6465E-05			
		3.8697E-05	2.1199E-05	1.0413E-05	5.0000E-06	2.6293E-06			
		1.5106E-06	5.0000E-07	2.0000E-07	1.0000E-07	0.			
		0.	0.	-1.0000E+00					
	WFN 6	1.0000E+02							
		-1.0000E+00	5.0000E-02	1.3488E-02	1.0148E-02	4.7609E-03			
ALTERED FROM 3.4489E-04		2.2000E-03	1.1949E-03	5.0000E-04	2.1723E-04	8.2253E-05			
		5.7428E-05	2.0000E-05	1.0432E-05	4.6621E-06	2.2761E-06			
		1.2537E-06	7.1526E-07	2.6978E-07	1.0000E-07	0.			
		0.	0.	-1.0000E+00					

THIS IS EXPLANATION FOR STRANGE BEHAVIOR IN TRACKS ENTERING

Fig. 40. Adjusted (by hand) space-energy weight window.

CELL PROGR	PROBL	TRACKS ENTERING	POPULATION	COLLISIONS	COLLISIONS * WEIGHT (PER HISTORY)	NUMBER WEIGHTED ENERGY	FLUX WEIGHTED ENERGY	AVERAGE TRACK WEIGHT (RELATIVE)	AVERAGE TRACK MFP (CM)
2	2	75839	74458	67419	2.5887E+00	7.9638E-01	1.6533E+00	1.4940E+00	5.0648E+00
3	3	14452	13526	23624	1.3723E+00	3.8601E-01	1.0408E+00	1.8806E+00	4.0246E+00
4	4	7094	11621	19613	4.4147E-01	3.2964E-01	1.0203E+00	6.7903E-01	3.9177E+00
5	5	6463	10463	17155	1.7049E-01	2.9225E-01	9.7468E-01	2.9678E-01	3.8096E+00
6	6	6025	8987	15519	5.3747E-02	2.9966E-01	1.1276E+00	1.0221E-01	3.9156E+00
7	7	5431	8875	14304	1.3574E-02	3.2879E-01	1.4363E+00	3.0759E-02	4.1831E+00
8	8	5290	8625	14496	5.0786E-03	3.4398E-01	1.6151E+00	1.1507E-02	4.3780E+00
9	9	5284	9240	16077	1.7477E-03	5.4043E-01	1.9626E+00	3.9657E-03	4.8172E+00
10	10	5604	9935	16767	7.2720E-04	5.4411E-01	2.0717E+00	1.5457E-03	4.8804E+00
11	11	5837	9861	16517	2.7529E-04	5.8899E-01	2.2996E+00	6.2135E-04	5.1875E+00
12	12	5865	9534	17366	1.1332E-04	6.4903E-01	2.4117E+00	2.5637E-04	5.3153E+00
13	13	6120	9832	18524	5.2946E-05	5.7115E-01	2.3792E+00	1.1583E-04	5.3554E+00
14	14	6243	9828	19735	2.4367E-05	6.7946E-01	2.3729E+00	5.1952E-05	5.3850E+00
15	15	6496	9846	20748	1.1101E-05	6.7425E-01	2.3827E+00	2.3384E-05	5.4389E+00
16	16	6904	10237	23801	5.0579E-06	7.1928E-01	2.3795E+00	1.0239E-05	5.5013E+00
17	17	7323	10736	29314	2.5555E-06	6.7818E-01	2.2056E+00	4.4929E-06	5.4331E+00
18	18	7585	11349	34042	1.1560E-06	6.5039E-01	2.1465E+00	1.8680E-06	5.3270E+00
19	19	5876	10556	30980	4.6402E-07	6.9589E-01	2.2556E+00	8.5181E-07	5.4331E+00
20	20	5424	5422	0	0.	1.2470E+00	3.5400E+00	6.8250E-07	1.0000+123
21	21	29	58	29	5.1765E-12	8.5566E-01	2.9814E+00	2.6879E-07	6.9683E+02
22	22	4	4	0	0.	2.6789E+00	2.8768E+00	1.3916E-08	1.0000+123
TOTAL		195188	252993	416030	4.6483E+00				

NPS	TALLY 1			TALLY 4			TALLY 5		
	MEAN	ERROR	FOM	MEAN	ERROR	FOM	MEAN	ERROR	FOM
4000	4.63475E-08	.2790	47	2.53090E-14	.8405	5	2.68446E-18	.9999	3
8000	4.37917E-08	.1876	56	1.26545E-14	.8406	2	1.34223E-18	.9999	1
12000	4.58544E-08	.1421	66	1.25263E-14	.6535	3	2.92610E-18	.7585	2
16000	4.32273E-08	.1230	67	1.08950E-14	.5801	3	2.19458E-18	.7585	1
20000	4.53445E-08	.1118	65	1.10367E-14	.4817	3	2.99296E-18	.6073	2
24000	4.80343E-08	.1006	66	1.07584E-14	.4246	3	3.64405E-18	.4737	3
28000	5.00952E-08	.0927	67	9.65057E-15	.4082	3	3.12347E-18	.4737	2
32000	4.87681E-08	.0870	67	8.44425E-15	.4082	3	2.73304E-18	.4737	2
36000	5.17198E-08	.0786	71	7.50600E-15	.4082	2	2.42937E-18	.4737	1
40000	5.43840E-08	.0729	73	9.64150E-15	.4140	2	2.60061E-18	.4289	2
44000	5.35161E-08	.0695	73	9.03835E-15	.4026	2	2.47533E-18	.4121	2
48000	5.22673E-08	.0669	74	8.28516E-15	.4026	2	2.26905E-18	.4121	1
52000	5.16625E-08	.0649	73	8.06101E-15	.3854	2	2.09451E-18	.4121	1
56000	5.20026E-08	.0627	73	7.90250E-15	.3689	2	1.94490E-18	.4121	1
60000	5.13074E-08	.0606	73	7.77769E-15	.3536	2	2.01116E-18	.3845	1
64000	5.05774E-08	.0589	72	7.88994E-15	.3312	2	2.03202E-18	.3640	1
68000	5.05022E-08	.0570	73	7.85279E-15	.3179	2	1.91249E-18	.3640	1
72000	5.10846E-08	.0552	73	8.63009E-15	.2822	2	2.20504E-18	.3182	2
74051	5.08709E-08	.0547	72	8.60730E-15	.2762	2	2.20049E-18	.3111	2

TIME = 4.60 MINUTES

← PERVERSELY THE FOM DECREASES, BUT NOT STATISTICALLY SIGNIFICANT

Fig. 41. Bad window corrected.

source particle. In contrast, a 14-MeV source particle will typically have higher energy in every part of the problem than a 2-MeV source particle would have. Thus the benefit of source energy biasing is felt throughout the entire problem, but the source angle biasing will be felt only within a few free paths of the source. Most of the sample problem is more than a few free paths from the source, so I would be surprised to see more than a 10% FOM improvement with *any* type of source angle bias.

XV. THE EXPONENTIAL TRANSFORM

The exponential transform in MCNP stretches distances between collisions in the forward direction and shrinks them in the backward direction by modifying the total macroscopic cross section by

$$\sigma_{\text{modified}} = \sigma_{\text{true}} (1 - p\mu)$$

$\mu = 1 \rightarrow$ forward direction,

where μ is the cosine of the angle with respect to a reference direction (currently only $+\hat{y}$ in MCNP) and p is the user input exponential transform parameter ($0 \leq p \leq 1$) with

$p = 0$ no bias
 $p = 1$ complete bias.

Many claims for the exponential transform exist in the Monte Carlo literature, but they are usually based on analysis of one-dimensional problems and often on one-dimensional monoenergetic problems. In practice at Los Alamos, the exponential transform is considered a dangerous biasing technique unless accompanied by weight control (for example, the weight window in MCNP). In fact, so many MCNP users had problems obtaining reliable mean and variance estimates with the exponential transform (when used without the weight window) that the technique was sometimes referred to as the "dial an answer technique."

Los Alamos experience indicates that the weight window eliminates the "dial an answer" phenomenon and that the exponential transform can be effective when used with a weight window. The exponential transform both with and without a weight window will be demonstrated on the sample problem.

A. Comments

1. MCNP gives a warning message if the exponential transform is used and a weight window is not.
2. The exponential transform is not recommended for novices.

3. The exponential transform works best in highly absorbing media and very poorly in highly scattering media.
4. Empirically, $p = 0.7$ seems to work well for shielding calculations on fission or fusion spectrums with shielding materials like concrete or earth.
5. There is a standard (maintained) patch to allow the reference direction to be arbitrary, not just $+\hat{y}$ as currently implemented.

B. The Sample Problem with the Exponential Transform

An exponential transform (with $p = 0.7$) was added to the input file that produced Fig. 42. That is, the following techniques were used in the next run:

1. energy cutoff,
2. forced collision in cell 21,
3. ring detector,
4. space-energy weight window,
5. source energy biasing, and
6. exponential transform ($p = 0.7$)

Figure 42 shows the results of using the exponential transform with a space-energy window; the FOM improved from 72 to 126. Results from running the same problem without the space-energy window are shown in Fig. 43. Note that the errors are much worse, and moreover, are not decreasing monotonically with increasing histories. Admittedly, the error levels are too high to make them reliable; however, one can certainly expect less jumpy statistics. For instance, compare tally 1 with tally 4 of the previous table. Note that even though the initial errors are high for tally 4, they are decreasing monotonically. Jumps in the relative errors indicate a few large weight particles trouncing the tally and thus indicate poor sampling. I have seen such relative error jumps frequently at the 10% level and occasionally at the 5% level. The higher the transform parameter is and the more collisions that are undergone per particle, the worse these jumps become. The weight window splits particles before their weights can become excessive enough to trounce the tallies.

Concerning tally 1 of Fig. 43, note that at 80,000 histories, the stated results are $2.75\text{E-}8 \pm 30.6\%$, yet Fig. 42 indicates that the true mean is close to $4.85\text{E-}8$. A quick calculation gives

$$\begin{aligned} \text{standard deviation} &= .306 \cdot 2.75\text{E-}8 &= 8.41 \text{E-}9 \\ \text{"true" - estimate} &= 4.85\text{E-}8 - 2.75\text{E-}8 &= 2.1\text{E-}8 \\ \text{standard deviations} & &= \frac{2.1\text{E-}8}{8.41\text{E-}9} = 2.5 \\ \text{from the true mean} & & \\ \text{ratio true/estimate} & &= 1.76, \end{aligned}$$

which indicates just how unreliable error estimates can be when the sampling is poor.

CELL PROGR	PROBL	TRACKS ENTERING	POPULATION	COLLISIONS	COLLISIONS * WEIGHT (PER HISTORY)	NUMBER WEIGHTED ENERGY	FLUX WEIGHTED ENERGY	AVERAGE TRACK WEIGHT (RELATIVE)	AVERAGE TRACK MFP (CM)
2	2	82381	82065	53810	2.6281E+00	8.2171E-01	1.7031E+00	1.6858E+00	7.9556E+00
3	3	19981	23648	25074	1.1835E+00	4.3859E-01	1.1523E+00	1.3032E+00	7.2574E+00
4	4	16444	18607	18914	5.0508E-01	3.0316E-01	9.4543E-01	6.6849E-01	6.6648E+00
5	5	13541	15386	15706	1.4711E-01	3.1359E-01	1.0435E+00	2.5234E-01	6.8687E+00
6	6	11461	13496	14039	4.0306E-02	3.3080E-01	1.2151E+00	8.5035E-02	7.2066E+00
7	7	10417	13454	13729	1.6137E-02	3.3603E-01	1.3958E+00	3.1007E-02	7.5390E+00
8	8	10189	13378	13591	4.8696E-03	3.9568E-01	1.6342E+00	1.0773E-02	8.1615E+00
9	9	10250	14088	14822	1.6739E-03	5.2252E-01	1.9818E+00	3.5829E-03	8.7372E+00
10	10	10659	13949	14231	5.8934E-04	6.1559E-01	2.3504E+00	1.3240E-03	9.4099E+00
11	11	10642	13602	14796	2.1034E-04	7.5516E-01	2.6706E+00	5.2503E-04	1.0151E+01
12	12	10527	14024	15551	9.9072E-05	8.1054E-01	2.6844E+00	2.3439E-04	1.0440E+01
13	13	10986	14644	17538	5.0323E-05	7.6932E-01	2.4881E+00	1.0879E-04	1.0112E+01
14	14	11539	15409	19466	2.5835E-05	6.5316E-01	2.2961E+00	5.0285E-05	9.7571E+00
15	15	12046	15625	21329	1.2003E-05	6.4574E-01	2.2270E+00	2.3125E-05	9.6251E+00
16	16	12356	15632	23077	5.2759E-06	6.8950E-01	2.3015E+00	1.0010E-05	9.9596E+00
17	17	12553	16094	28198	2.6284E-06	6.7305E-01	2.1726E+00	4.5005E-06	9.6617E+00
18	18	13192	16913	32669	1.1979E-06	6.2959E-01	2.1103E+00	1.9486E-06	9.6765E+00
19	19	11444	16369	31267	4.7481E-07	6.5745E-01	2.1606E+00	8.5094E-07	1.0147E+01
20	20	11122	11101	0	0.	1.2966E+00	3.4708E+00	3.2605E-07	1.0000+123
21	21	97	194	100	5.4336E-12	2.1163E+00	4.2544E+00	9.7467E-08	7.7796E+02
22	22	11	11	0	0.	3.8622E+00	4.0376E+00	3.1275E-09	1.0000+123
TOTAL		301838	357689	387907	4.5278E+00				

NOTE IMPROVEMENT

NPS	TALLY 1			FOM	TALLY 4			FOM	TALLY 5			FOM
	MEAN	ERROR	FOM		MEAN	ERROR	FOM		MEAN	ERROR	FOM	
4000	4.47297E-08	.1825	119	1.18956E-14	.6162	10	1.03622E-17	.5654	12			
8000	4.70824E-08	.1307	121	1.11439E-14	.4389	10	6.52695E-18	.4726	9			
12000	5.14633E-08	.0996	138	8.94383E-15	.3784	9	5.17462E-18	.4082	8			
16000	4.66144E-08	.0894	139	8.73207E-15	.3215	10	5.38702E-18	.3371	9			
20000	4.82730E-08	.0813	133	1.02135E-14	.3102	9	5.76006E-18	.2992	9			
24000	5.00965E-08	.0731	134	1.14411E-14	.2876	8	5.41260E-18	.2795	9			
28000	4.84900E-08	.0680	135	1.10845E-14	.2689	8	4.77614E-18	.2723	8			
32000	4.81146E-08	.0643	133	1.06399E-14	.2541	8	4.29410E-18	.2657	7			
36000	4.89508E-08	.0597	135	1.15818E-14	.2237	9	4.82404E-18	.2366	8			
40000	4.85085E-08	.0575	132	1.20101E-14	.2095	10	4.92557E-18	.2259	8			
44000	4.74248E-08	.0550	134	1.10572E-14	.2073	9	4.55676E-18	.2226	8			
48000	4.90814E-08	.0529	131	1.11509E-14	.1962	9	4.62668E-18	.2103	8			
52000	4.94231E-08	.0512	129	1.10281E-14	.1888	9	4.73347E-18	.1993	8			
56000	4.84339E-08	.0497	127	1.13865E-14	.1802	9	4.91778E-18	.1882	8			
60000	4.78067E-08	.0481	128	1.07393E-14	.1786	9	4.61025E-18	.1875	8			
64000	4.79871E-08	.0463	129	1.03275E-14	.1752	9	4.55199E-18	.1830	8			
68000	4.85386E-08	.0447	129	1.03254E-14	.1725	8	4.42669E-18	.1787	8			
72000	4.80605E-08	.0440	127	9.75179E-15	.1725	8	4.18076E-18	.1787	7			
76000	4.77400E-08	.0427	128	1.06664E-14	.1581	9	4.48125E-18	.1689	8			
80000	4.85226E-08	.0417	126	1.06919E-14	.1512	9	4.68326E-18	.1623	8			
81021	4.85159E-08	.0413	126	1.05571E-14	.1512	9	4.62424E-18	.1623	8			

DUMP NO. 2 ON FILE RUNTPF NPS = 81021 CTM = 4.60

Fig. 42. Exponential transform added to window and source energy biasing.

XVI. THE GRAND FINALE—TURNING DXTRAN BACK ON

Recall that DXTRAN was turned off while the space-energy window and the exponential transform optimized the penetration. Figure 44 shows the results of turning DXTRAN back on. This “best” run uses

1. energy cutoff,
2. forced collision in cell 21,
3. ring detector,
4. space-energy weight window,
5. source energy biasing,
6. exponential transform ($p = 0.7$), and
7. DXTRAN with DXCPN card.

As observed previously, DXTRAN vastly improves tallies 4 and 5 at some expense to tally 1.

XVII. CORRELATED SAMPLING AND PERTURBATION CAPABILITY

A standard MCNP perturbation patch allows up to three slightly different Monte Carlo problems to be run simultaneously. The perturbation calculation estimates the difference in tallies between similar Monte Carlo problems and it estimates the standard tallies.*

Another way of estimating perturbations is correlated sampling in MCNP that allows tally differences to be estimated between two different runs by correlating their random number sequences. The i^{th} particle in run #2 is started with the same random number that starts the i^{th} particle in run #1. Because the i^{th} particle in run #1 might use k_1 random numbers, and the i^{th} particle in run #2 might use $k_2 \neq k_1$, random numbers, the $i + 1^{\text{st}}$ particle does not start with the next random number in the sequence after the i^{th} particle terminates. Instead, the $i + 1^{\text{st}}$ particle starts with the J^{th} random number beyond the starting random number for the i^{th} random number. In other words, there is a random number jump of J random numbers between the start of particle i and the start of particle $i + 1$. Thus the i^{th} particle in runs #1 and #2 will both be starting at the $(i - 1) \cdot J$ position in the random number sequence. J , of course, should be large enough so that both k_1 and k_2 are less than J for all particle histories. This correlation of random number sequences is depicted in Table IV.

*For further information, refer to video reel #24, “Various MCNP Patches, Column Input, Exponential Transform, Importance Generator, Perturbation,” by Robert G. Schrandt, from MCNP Workshop, Los Alamos National Laboratory, October 4-7, 1983. Available from Radiation Shielding Information Center, Oak Ridge National Laboratory, Oak Ridge, TN 37830.

The correlated sampling problem is identical to the sample problem except that the density in cell 21 (Fig. 3) has been changed. The two correlated problems have

1. density in cell 21 = $2.03\text{E-}4$ and
2. density in cell 21 increased by 1% to $2.0503\text{E-}4$.

Figure 45 summarizes the two problems, each run for 20,000 histories. Everything is identical between the two summary charts up to cell 21 because all particles have exactly the same random walk until they enter that cell. Furthermore, a particle entering cell 21, where the random walks diverge, will probably never scatter back toward cell 19. Presumably, if enough particles were run, backscatter from cell 21 would cause very small differences in cells 1-19.

Figure 46 shows FOM tables for the two problems. Note that the means differ by about 1% and that this difference appears to be statistically insignificant because of the 9% errors in the means. However, these charts can be used to obtain batch statistics on 20 batches of 1000. That is to say, the numbers can be postprocessed to figure out the tally for each batch of 1000 particles and then the difference in tally for each batch of 1000 particles can be computed. Error estimates in the tally difference can then be made on the basis of the 20 tally differences. Figure 47 shows the 20 means for each problem and the mean and relative error of the difference. Note that with correlated sampling, a 1% difference has been found to within 8% despite a 9% error in each of the problems.

XVIII. PHOTONS

The sample problem described here is a neutron-only problem. Regarding the variance reduction techniques in MCNP, whatever can be done for neutrons can be done for photons. Only the neutron-induced gamma problem needs special consideration. The difficulty arises in setting reasonable parameters (PWT card) to decide when a photon should be produced at a neutron collision. These parameters specify, on a cell-by-cell basis, the minimum weight for producing a photon. This weight should be inversely proportional to the cells' photon importance. One either has to make a guess or obtain an adjoint solution, such as provided by the weight window generator. In fact, if a photon weight window is used, these (PWT) parameters should be chosen as the lower weight bounds for the most important particles (typically the highest-energy window).

XIX. FUTURE PLANS

Goals for the future are

1. more automatic biasing (learning techniques),

TABLE IV. Random Number Usage in Correlated Runs

Random Numbers for Run #1 (* indicates the random number was actually used)	Random Numbers for Run #2 (* indicates the random number was actually used)
0.14784 * first particle starts here	0.14784 *
0.29376 *	0.29376 *
0.21632 *	0.21632 *
0.78048	0.78048 *
0.14336	0.14336 *
0.10304	0.10304
0.66592	0.66592
0.38144 * second particle starts here	0.38144 *
0.52416 *	0.52416 *
0.22912 *	0.22912 *
0.03968	0.03968
0.15776	0.15776
0.14464	0.14464
0.25248	0.25248
0.46272 * third particle starts here	0.46272 *
0.75904 *	0.75904

2. weight window and generator in more arbitrary phase space,
3. several random number generators (tallies should not affect random walks, and mode 1 neutrons should track mode 0 neutrons), and
4. more perturbation capability.

XX. CONCLUSION

The Los Alamos Monte Carlo neutron/photon particle transport code, MCNP, contains many effective variance reduction capabilities. However, these tech-

niques must be used judiciously and their effects must be monitored using the summary information provided by a Monte Carlo run. This paper has illustrated most of the MCNP variance reduction techniques on a conceptually simple, yet computationally demanding, neutron transport problem. These illustrations should help novice users better understand the capabilities of MCNP techniques more concretely than presented in the MCNP manual, which I hope this report will complement. Whereas the MCNP manual must be complete and general, this report makes no attempt to be either. Use this report to get a flavor for MCNP and the manual to set up problems.

$\rho = 2.03E-4$

CELL PROGR	TRACKS ENTERING PROBL	POPULATION	COLLISIONS	COLLISIONS * WEIGHT (PER HISTORY)	NUMBER WEIGHTED ENERGY	FLUX WEIGHTED ENERGY	AVERAGE TRACK WEIGHT (RELATIVE)	AVERAGE TRACK MFP (CM)
2	2	20310	20245	13230	2.9038E+00	7.8576E-01	1.8336E+00	7.7302E+00
3	3	4854	5773	6121	1.2068E+00	3.2962E-01	1.2787E+00	7.1288E+00
4	4	3983	4493	4395	2.0630E-01	5.6021E-01	1.4968E+00	8.9520E+00
5	5	3241	3709	3566	9.5539E-02	3.8258E-01	1.3786E+00	7.9343E+00
6	6	2762	3309	3316	2.8814E-02	4.3184E-01	1.5712E+00	8.1847E+00
7	7	2532	3204	3194	1.3999E-02	5.5666E-01	1.5506E+00	8.0382E+00
8	8	2463	3233	3286	5.1721E-03	3.6626E-01	1.5002E+00	8.0029E+00
9	9	2447	3364	3416	1.1440E-03	7.7182E-01	2.3990E+00	9.9393E+00
10	10	2596	3356	3506	8.1792E-04	5.8220E-01	1.9761E+00	8.7167E+00
11	11	2628	3430	3916	5.1950E-04	4.6087E-01	1.6235E+00	8.1114E+00
12	12	2668	3595	4368	2.4198E-04	4.1003E-01	1.4915E+00	7.7865E+00
13	13	2789	3740	4692	7.7618E-05	4.8312E-01	1.8747E+00	8.9391E+00
14	14	2911	3895	5208	3.2070E-05	5.3047E-01	2.0756E+00	9.1714E+00
15	15	3017	4004	5647	1.2871E-05	5.9777E-01	2.2049E+00	9.5372E+00
16	16	3154	4178	6746	5.7756E-06	6.8805E-01	2.3307E+00	9.8171E+00
17	17	3339	4116	6794	2.4249E-06	6.7461E-01	2.2597E+00	9.8965E+00
18	18	3318	4277	8139	1.1850E-06	6.7566E-01	2.1622E+00	9.6692E+00
19	19	2847	4074	7528	4.5173E-07	6.7608E-01	2.2620E+00	1.0292E+01
20	20	6112	16583	0	0.	1.2958E+00	3.4588E+00	1.0000+123
21	21	13803	27610	13805	4.7205E-14	1.8236E+00	4.4833E+00	7.6105E+04
22	22	1348	1348	0	0.	3.4188E+00	7.1054E+00	2.4142E-12
TOTAL		93122	131536	110873	4.4633E+00			

DID THE SAME THINGS UNTIL ENTERING THE PERTURBED
REGION BECAUSE THE RANDOM NUMBERS WERE THE SAME

 $\rho = 2.0503E-4$

CELL PROGR	TRACKS ENTERING PROBL	POPULATION	COLLISIONS	COLLISIONS * WEIGHT (PER HISTORY)	NUMBER WEIGHTED ENERGY	FLUX WEIGHTED ENERGY	AVERAGE TRACK WEIGHT (RELATIVE)	AVERAGE TRACK MFP (CM)
2	2	20310	20245	13230	2.9038E+00	7.8576E-01	1.8336E+00	7.7302E+00
3	3	4854	5773	6121	1.2068E+00	3.2962E-01	1.2787E+00	7.1288E+00
4	4	3983	4493	4395	2.0630E-01	5.6021E-01	1.4968E+00	8.9520E+00
5	5	3241	3709	3566	9.5539E-02	3.8258E-01	1.3786E+00	7.9343E+00
6	6	2762	3309	3316	2.8814E-02	4.3184E-01	1.5712E+00	8.1847E+00
7	7	2532	3204	3194	1.3999E-02	5.5666E-01	1.5506E+00	8.0382E+00
8	8	2463	3233	3286	5.1721E-03	3.6626E-01	1.5002E+00	8.0029E+00
9	9	2447	3364	3416	1.1440E-03	7.7182E-01	2.3990E+00	9.9393E+00
10	10	2596	3356	3506	8.1792E-04	5.8220E-01	1.9761E+00	8.7167E+00
11	11	2628	3430	3916	5.1950E-04	4.6087E-01	1.6235E+00	8.1114E+00
12	12	2668	3595	4368	2.4198E-04	4.1003E-01	1.4915E+00	7.7865E+00
13	13	2789	3740	4692	7.7618E-05	4.8312E-01	1.8747E+00	8.9391E+00
14	14	2911	3895	5208	3.2070E-05	5.3047E-01	2.0756E+00	9.1714E+00
15	15	3017	4004	5647	1.2871E-05	5.9777E-01	2.2049E+00	9.5372E+00
16	16	3154	4178	6746	5.7756E-06	6.8805E-01	2.3307E+00	9.8171E+00
17	17	3339	4116	6794	2.4249E-06	6.7461E-01	2.2597E+00	9.8965E+00
18	18	3318	4277	8139	1.1850E-06	6.7566E-01	2.1622E+00	9.6692E+00
19	19	2847	4074	7528	4.5173E-07	6.7608E-01	2.2620E+00	1.0292E+01
20	20	6112	16583	0	0.	1.2958E+00	3.4588E+00	1.0000+123
21	21	13803	27610	13805	4.7677E-14	1.8236E+00	4.4832E+00	7.5351E+04
22	22	1348	1348	0	0.	3.4173E+00	7.1042E+00	2.4147E-12
TOTAL		93122	131536	110873	4.4633E+00			

Fig. 45. Correlated sampling example.

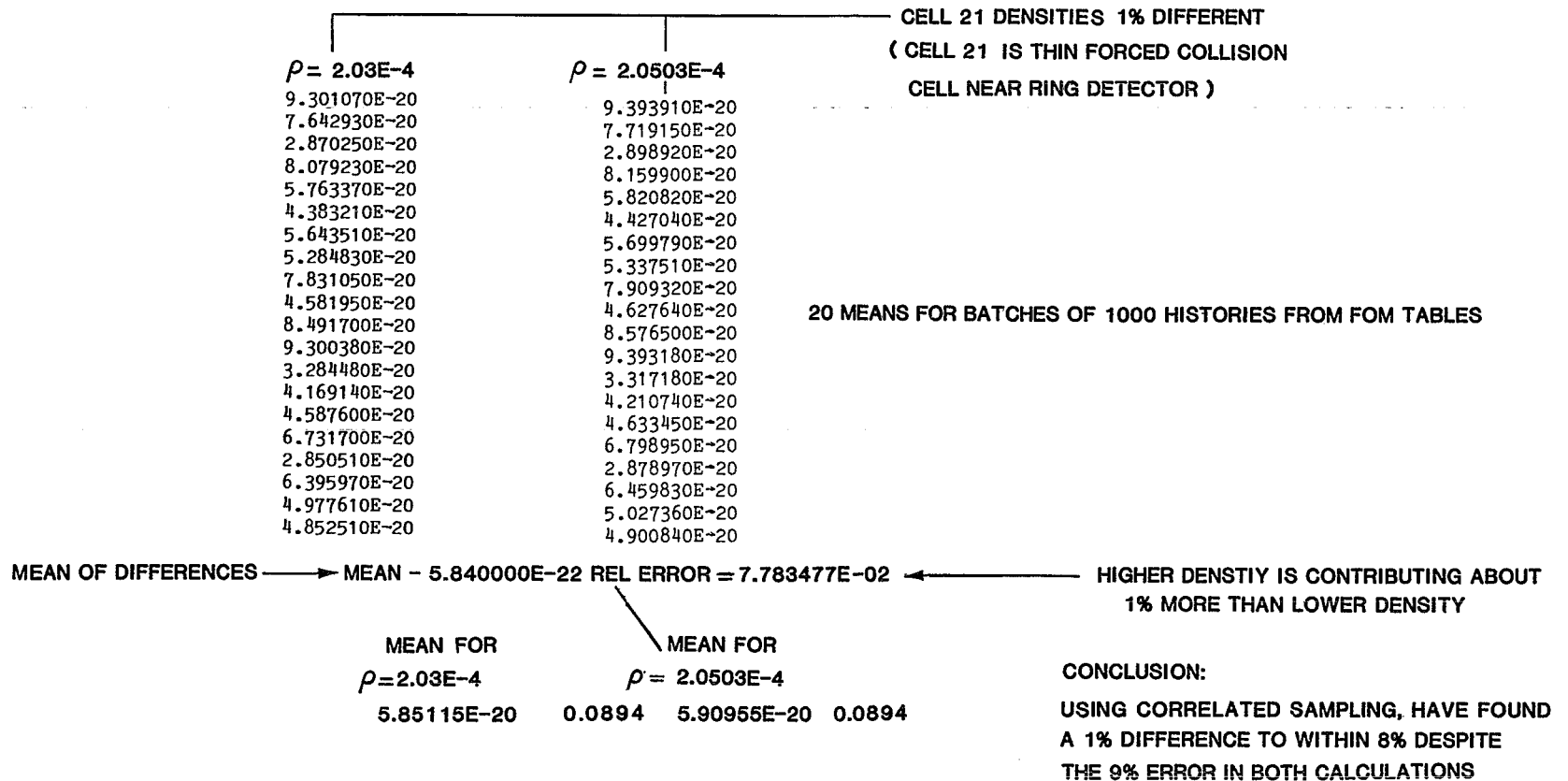


Fig. 47. Means for standard density and perturbed density problems.

XXI. SUMMARY

SUMMARY PROBLEM #1

Page This Report	Techniques	Particles Time Part/Min	F1 σ_{mr} FOM	F4 σ_{mr} FOM	F5 σ_{mr} FOM	Comments
6	Analog	3919 0.61 min 6425	0	0	0	No particles get past cell 14 (Point detector contributions only from cell 21).
8	Energy Cutoff .01 MeV	13968 0.60 min 23280	0	0	0	Assumes particles below .01 MeV do not contribute; No particles beyond cell 13.
11	Geometry Splitting (factor of 2, cells 2-19) Energy Cutoff	2118 0.60 min 3530	5.87E-7 0.24 27	0	0	Particles now penetrating concrete; use "tracks entering" to refine importances.
12	Refined Splitting Energy Cutoff	1520 0.58 min 2620	5.03E-7 0.27 23	7.21E-14 1.00 1	0	Keep refined splitting on "tracks entering" information.
14	Energy Roulette Refined Splitting Energy Cutoff	4699 0.61 min 7703	8.38E-7 0.18 50	1.92E-13 0.64 4	0	Factor of 2 gained by energy roulette.
17	Weight Cutoff/ Implicit Capture Energy Roulette Refined Splitting Energy Cutoff	2099 0.61 min 3441	5.62E-7 0.19 37	5.59E-14 0.73 2	0 0	Implicit capture and weight cutoff did reduce the history variance, but time per history increased too much. Thus analog capture better.
19	Forced Collision Energy Roulette Refined Splitting Energy Cutoff	31617 4.61 min 6858	5.59E-7 0.068 45	7.53E-14 0.27 2	2.61E-17 0.29 2	Forced collision allows the point detector (F5) to get tallies. Material too thin.
25	DXTRAN Forced Collision Energy Roulette Refined Splitting Energy Cutoff	2231 1.43 min 1560	7.35E-7 0.23 12	1.24E-13 0.21 15	7.62E-17 0.22 14	DXTRAN successful for tallies 4 and 5, but too slow; angle biasing definitely helps, work on speed.
26	DXCPN and DXTRAN Forced Collision Energy roulette Refined Splitting Energy Cutoff	11427 2.60 min 4395	7.32E-7 0.10 34	1.22E-13 0.095 42	7.21E-17 0.10 34	DXCPN solves speed problem. Note F1 tally $4395/1560 \approx 34/12 = \text{FOM ratio}$.

PROBLEM #1 (continued)

Page This Report	Techniques	Particles Time Part/Min	F1 σ_{mr} FOM	F4 σ_{mr} FOM	F5 σ_{mr} FOM	Comments
27	Ring Detector	11755	6.54E-7	1.16E-13	6.78E-17	Ring detector looks marginally better.
	Energy Roulette	2.60 min	0.10	0.093	0.096	
	DXTRAN/DXCPN	4521	38	44	41	
	Forced Collision Refined Splitting Energy Cutoff					
30	Cone Biasing	6049	6.82E-7	1.22E-13	7.37E-17	Cone bias has little effect because $-\hat{y}$ source particles die quickly. Remove cone bias below.
	Ring Detector	2.60 min	0.11	0.092	0.097	
	DXTRAN/DXCPN	2327	32	45	40	
	Forced Collision Refined Splitting Energy Cutoff					
	Energy Roulette					
32	Exponential Bias	5404	6.79E-7	1.05E-13	6.43E-17	Exponential source bias looks marginally detrimental.
	Ring Detector	2.59 min	0.11	0.098	0.10	
	DXTRAN/DXCPN	2086	33	39	35	
	Forced Collision Refined Splitting Energy Roulette					
	Energy Cutoff					

SUMMARY PROBLEM #2
New Source 95% at 2 MeV and 5% at 14 MeV

Page This Report	Techniques	Particles Time Part/Min	F1 σ_{mr} FOM	F4 σ_{mr} FOM	F5 σ_{mr} FOM	Comments
33	Splitting (same) Energy Cutoff, Ring Detector/Forced Collision/DXTRAN/ DXCPN (subsequent runs use above tech- niques unless speci- fied otherwise)	33092 4.60 min 7194	4.43E-8 0.23 4	7.57E-15 0.22 4	4.35E-18 0.21 4	Problem much harder because source spectrum much softer. Factor 15 less transmission.
35	Source Energy Bias	6306 4.63 min 1362	4.90E-8 0.11 16	8.61E-15 0.11 17	5.10E-18 0.11 17	Factor of four improvement by E bias.
36	No source energy bias, energy roulette	66475 4.61 min 14420	6.22E-8 0.15 9	9.80E-15 0.14 10	5.94E-18 0.15 9	Worse than source energy bias, better than <i>no</i> energy discrimination.
39	Source Energy Bias Energy Roulette	16957 4.61 min 3678	5.04E-8 0.080 33	8.81E-15 0.76 37	5.14E-18 0.076 38	Good idea to use both in this problem.
42	Turn off splitting and use importances as weight window	46770 4.60 min 10167	5.87E-8 0.27 3	1.05E-14 0.24 3	5.82E-18 0.23 3	Within statistics, about the same as splitting.

Subsequent Runs Use Weight Window Unless Otherwise Specified

Page This Report	Techniques	Particles Time Part/Min	F1 σ_{mr} FOM	F4 σ_{mr} FOM	F5 σ_{mr} FOM	Comments
45	Window from importance generator on (spatial)	46770 4.79 min 9764	5.87E-8 0.27 2	1.05E-8 0.24 3	5.82E-18 0.23 3	Note this run and previous run tracked; only difference is a 4% reduction in speed.
48	Use generated space window, turn DXTRAN off, space-energy generator on	28144 4.63 6079	3.66E-8 0.19 6	5.08E-15 0.66 0	1.96E-18 0.76 0	DXTRAN turned off while window is being optimized for penetration.
50	Space-energy window generated above; DXTRAN off	79266 4.61 min 17194	4.48E-8 0.070 43	8.24E-15 0.23 4	4.24E-18 0.26 4	Space-energy window gives dramatic improvement.
51	Source energy bias so that particles start within space-energy window	71167 4.61 min 15438	4.92E-8 0.054 75	8.48E-15 0.29 2	9.20E-18 0.51 0	Note good improvement with source energy bias.
53	Same as above, except correct bad window	74051 4.60 min 16098	5.09E-8 0.55 72	8.61E-15 0.28 2	2.20E-18 0.31 2	Murphy's Law.
55	Exponential transform, space-energy window, source-energy bias	81021 4.60 min 17613	4.85E-8 0.041 126	1.06E-14 0.15 9	4.62E-18 0.16 8	Exponential transform works well with weight window.
56	Same as above, except remove window	90897 4.60 min 19760	4.05E-8 0.35 1	1.90E-16 1 0	8.59E-20 1 0	Exponential transform <i>requires</i> window.
59	GRAND FINALE Turn DXTRAN back on	51909 4.60 min 11285	4.74E-8 0.053 77	8.46E-15 0.055 71	4.86E-18 0.054 73	

REFERENCES

1. Los Alamos Monte Carlo Group, "MCNP—A General Monte Carlo Code for Neutron and Photon Transport," Los Alamos National Laboratory report LA-7396-M (Rev.) (April 1981).
2. Thomas E. Booth, "Monte Carlo Variance Comparison for Expected Value Versus Sampled Splitting," *Nuclear Science and Engineering* 89, 305-309 (1985).

APPENDIX

Input File Differences for MCNP Version 3A

The calculations described in this report were done with MCNP version 2D, and some of the input file specifications have been changed in version 3A. This appendix was added to aid the reader who wants to run the sample problem on MCNP3A.

The source specification (cards SRC1, SI, and SP of Fig. 2) will have to be altered substantially. In addition, the reader should be aware of the following changes:

1. Particle Types:

MCNP3A will recognize two particle types with the following mnemonics:

N = neutron
P = photon

2. Data Cards:

The particle type of each data card will be the first data entry and no longer appear as part of the data card name. This means that the following data cards are renamed:

New Name	Old Name(s)	Description
IMP	IN,IP	importance
CUT	CUTN,CUTP	time, energy, weight cutoffs
PHYS	ERGN,ERGP	energy physics cutoffs
WWN	WFN,WFP	weight window bounds
WWE	WFN,WFP	weight window energies
WWGE	WGEN,WGEP	weight window generator energies
WWP	WDWN,WDWP	weight window game parameters
ESPLT	NSPLT,PSPLT	energy splitting/roulette
EXT	EXTYN,EXTYP	exponential transform
DXT	DXN,DXP	DXTRAN sphere specification
FCL	FCN,FCP	forced collisions
DXC	DXCPN,DXCPP	DXTRAN cell contributions

The new root entry will appear in columns 1-5; the N or P data type will be the first entry beyond column 5. If the first data entry is not an N or P, there will be a fatal error. Note that only one particle type may be specified. If the particle type is inconsistent with the problem mode, there will be a warning error. A warning rather than a fatal error will be issued so that a coupled neutron/photon run may be switched to a neutron-only run without removing all the photon data cards. In MCNP3A the old data cards will be accepted with a warning that they will be obsolete in MCNP3B.

3. MODE Card:

The MODE card will specify the problem particle types. Examples:

```
MODE N           (old mode 0)
MODE N P        (old mode 1)
MODE P N        (old mode 1)
MODE P          (old mode 2)
```

If both N and P are specified, the order does not matter for MCNP3A and the two entries must be separated by at least one space. The space is required so that future versions of the code can have particle types with more than one character mnemonics.

The old MODE card will be accepted with a warning that it will have different entries in MCNP3B.

4. Tally Particle Types:

Whether a tally is a neutron or photon tally is specified by an N or P as the first entry on the tally Fn card regardless of the tally number. For MCNP3A, if the N or P is missing then a warning will be issued and the particle type will be assumed from the tally number as in previous versions. Examples:

```
F4   P c1 c2 c3   photon flux tally
F15  N x y z ro   neutron detector tally
F7   c1 c2 c3     neutron heating tally:
                    warning issued.
```


The neutron and photon heating tallies may be added together by having both an N and a P as the first and second data entries. The N and P may be in any order, i.e., P and N, and they must be separated by a space. The F6 and F16 tally types are the only tally types that may be added in this way. A corresponding FMn card for the combined tally causes

a fatal error if it contains anything more than constants. Examples of proper usage:

```
F6      P N c1 c2 c3
FM6     C1

F36     N P c1 c2 c3 c4
FM36   (C1) (C2) (C3) (C4) (C5)
```

This report has been reproduced directly from the best available copy.

It is available to DOE and DOE contractors from the Office of Scientific and Technical Information, P.O. Box 62, Oak Ridge, TN 37831. Prices are available from (615) 576-8401.

It is available to the public from the National Technical Information Service, US Department of Commerce, 5285 Port Royal Rd. Springfield, VA 22161.

